

**TNO report****TNO 2017 R11014****Velmod-3.1****Earth Life and Social Sciences**

Princetonlaan 6  
3584 CB Utrecht  
P.O. Box 80015  
3508 TA Utrecht  
The Netherlands

[www.tno.nl](http://www.tno.nl)

T +31 88 866 42 56

Date	7 november 2017
Author(s)	M.P.D. Pluymaekers, J.C. Doornenbal and H. Middelburg
Copy no	
No. of copies	
Number of pages	66 (incl. appendices)
Number of appendices	5
Sponsor	
Project name	GIP 2017 - Kartering Diepe Ondergrond
Project number	060.26839

All rights reserved.

No part of this publication may be reproduced and/or published by print, photoprint, microfilm or any other means without the previous written consent of TNO.

In case this report was drafted on instructions, the rights and obligations of contracting parties are subject to either the General Terms and Conditions for commissions to TNO, or the relevant agreement concluded between the contracting parties. Submitting the report for inspection to parties who have a direct interest is permitted.

© 2017 TNO

# Contents

<b>1</b>	<b>Introduction .....</b>	<b>3</b>
<b>2</b>	<b>Data .....</b>	<b>4</b>
2.1	Velocity data .....	4
2.2	Deviation data .....	4
2.3	Lithostratigraphic marker data .....	4
2.4	Data quality control and normalization .....	4
<b>3</b>	<b>VELMOD velocity models .....</b>	<b>6</b>
3.1	Layer cake model .....	6
3.2	Compacting layers .....	6
3.3	Model parameterization .....	6
3.4	Zechstein and other groups .....	17
<b>4</b>	<b>Results .....</b>	<b>21</b>
4.1	Spatial data analysis .....	21
4.2	Regional $V_{int}$ distribution maps .....	21
4.3	Regional $V_0$ distribution maps .....	37
4.4	T/Z pairs .....	51
<b>5</b>	<b>Discussion and recommendations .....</b>	<b>52</b>
5.1	Data reliability .....	52
5.2	Spatial velocity distributions .....	52
5.3	Model parametrization .....	52
5.4	Velocity model .....	53
5.5	Geological aspects .....	53
<b>6</b>	<b>References .....</b>	<b>54</b>
<b>7</b>	<b>Signature .....</b>	<b>55</b>
	<b>Appendices</b>	
	A Velocity borehole data files	
	B Velocity model well results	
	C $V_{int}$ , $V_0$ & kriging standard deviation grids	
	D T/Z pairs	
	E Analysis of regional $V_{int}$ variations	

# 1 Introduction

VELMOD-3 is the successor of VELMOD-2, a seismic velocity model that was built in the context of a Joint Industry Project (van Dalfsen et al, 2007). This model, as well as the previous models, are based on velocity data from sonic logs and checkshot data to which depth markers of lithostratigraphic layer boundaries had been assigned. With this data a *layer-cake* velocity model is constructed based on  $V0-k$  parameterization.

The primary application of the VELMOD-3 model is time-depth conversion for large scale (regional) seismic interpretation and mapping.

In comparison with its predecessor, VELMOD-3 had more digital sonic data of much more boreholes at its disposal (1642 compared to 1383). Enlargement of the digital sonics database was effected by data release of E&P companies in the context of the mining law.

## 2 Data

### 2.1 Velocity data

The used velocity dataset consists of sonic logs and checkshot data. Sonic data from different logging tools was available, often expressed in different formats like slowness, instantaneous sonic velocity and (calibrated) travelttime-depth (TZ) pairs. The dataset comprises (digital available) data of well released to the public domain before September 1<sup>st</sup> 2012. All borehole data files used within this project are listed in appendix B.

### 2.2 Deviation data

All used deviation data were available from DINO (the National Geo-data Centre of the Netherlands), through the 'NL Olie- en Gasportaal' at [www.nlog.nl](http://www.nlog.nl).

### 2.3 Lithostratigraphic marker data

Borehole lithostratigraphic marker data were retrieved from DINO. These markers are assigned conform the standard stratigraphic nomenclature of the Netherlands (Van Adrichem Boogaert & Kouwe, 1993-1997). The lithostratigraphic data was aggregated from stratigraphic member level to main stratigraphic (sub) group level (Figure 2).

### 2.4 Data quality control and normalization

All raw velocity data was subject to quality control in terms of (velocity) data type and accompanying data unit. Per well the dataset was checked on completeness. Wells without stratigraphic information were discarded. Wells without deviation data were considered to be vertical. The aggregated stratigraphic data was QC-ed on completeness and updated when necessary.

All velocity dataset were normalized to TVDSS (m), time (s), velocity (m/s). Duplicate depth/time values were removed. Datasets wit depth and/or time reversals (mainly checkshot data) were discarded from analysis. All normalized velocity data was stored in a database together with metadata, deviation data and stratigraphic data from the wells.

The data processing and QC is summarized in Figure 1



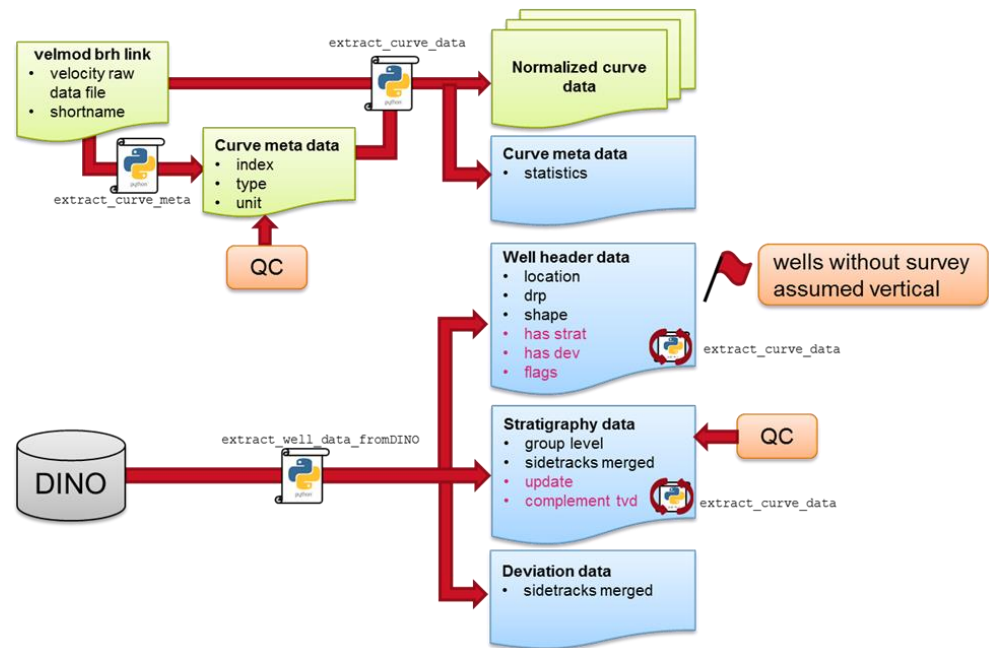


Figure 1 Overview of data processing workflow

### 3 VELMOD velocity models

#### 3.1 Layer cake model

Within this project a 'layer cake' type velocity model is used. For each defined stratigraphic layer (Figure 2) seismic velocity is modelled. Nine main stratigraphic units are distinguished.

- Three layers (1, 3 and 6) were split into two sublayers and also modelled individually.
- Only the Zechstein Group (layer 7 in Figure 2) was modelled with a different method (see 3.2).
- For the Limburg Group also the Geul Subgroup (DCG) was modelled individually.

#### 3.2 Compacting layers

Except the layer of the Zechstein Group (Figure 2, layer 7), all layers have been subjected to considerable compaction due to sediment loading during burial phases. This compaction resulted in an increase of compressional wave velocity of layer sediments with burial depth.

For the compacting layers, we adopt model velocities that increase linearly with depth. A velocity model of this type is completely described by:

$$V = V_0 + k Z \quad (\text{eq. 1})$$

Where  $V$  [m/s] is the instantaneous velocity,  $V_0$  [m/s] the normalized velocity,  $k$  [m/s/m] the velocity-depth gradient and  $Z$  [m] the depth.

#### 3.3 Model parameterization

The  $V_0$  and  $k$  model parameters were determined according to the  $V_{\text{int}} - Z_{\text{mid}}$  method applied per stratigraphic layer. This method approximates the regional velocity-depth gradient, as well as a regional normalized velocity. In figure 3 all interval velocity values ( $V_{\text{int}}$ ) for all lithostratigraphic groups except Zechstein Group have been plotted against the mid depth ( $Z_{\text{mid}}$ ). From this figure could be clearly concluded that there is a general increase of velocity with depth but also that the values per interval

Era	Period	Lithostratigraphy		Sublayers	Main layers	Lithology
CENOZOIC	Neogene	Upper North Sea Group – NU		a	1	Clays, silts, fine- to coarse-grained sands and sandstones
	Paleogene	Middle North Sea Group – NM		b		
		Lower North Sea Group – NL				
MESOZOIC	Cretaceous	Chalk Group – CK			2	Mainly limestones (chalk), also marls and claystones
		Rijnland Group – KN	Holland Formation – KNGL	a	3	Argillaceous and marly deposits, sandstone beds
			Vlieland subgroup – KNN	b		
	Jurassic	Schieland Group SL	Schieland, Scruff and Niedersachsen groups SL, SG, SK		4	Claystones, sandstones, limestones, evaporites and coal seams
		Altena Group – AT			5	Argillaceous deposits with calcareous intercalations and clastic sediments
		Triassic	Upper Germanic Trias Group – RN		a	6
	Lower Germanic Trias Group – RB		b			
PALEOZOIC	Permian	Zechstein Group – ZE			7	Evaporites and carbonates
		Upper Rotliegend Group – RO			8	Coarse and fine-grained clastic sediments
		Lower Rotliegend Group – RV				
	Carboniferous	Limburg Group – DC			9	Fine-grained siliciclastic sediments and coal seams
		Carboniferous Limestone Group – CL				

Figure 2 Layer cake model of VELMOD-3 based on lithostratigraphy after Van Adrichem Boogaert and Kouwe (1993-1997)

could be grouped or characterised by a certain dip ( $k$  value) and a certain  $v_0$  value: see for example the clear differences in the North Sea Supergroup values (yellow), Chalk Group (light green), Rijnland Group (dark green) and most of the other groups.

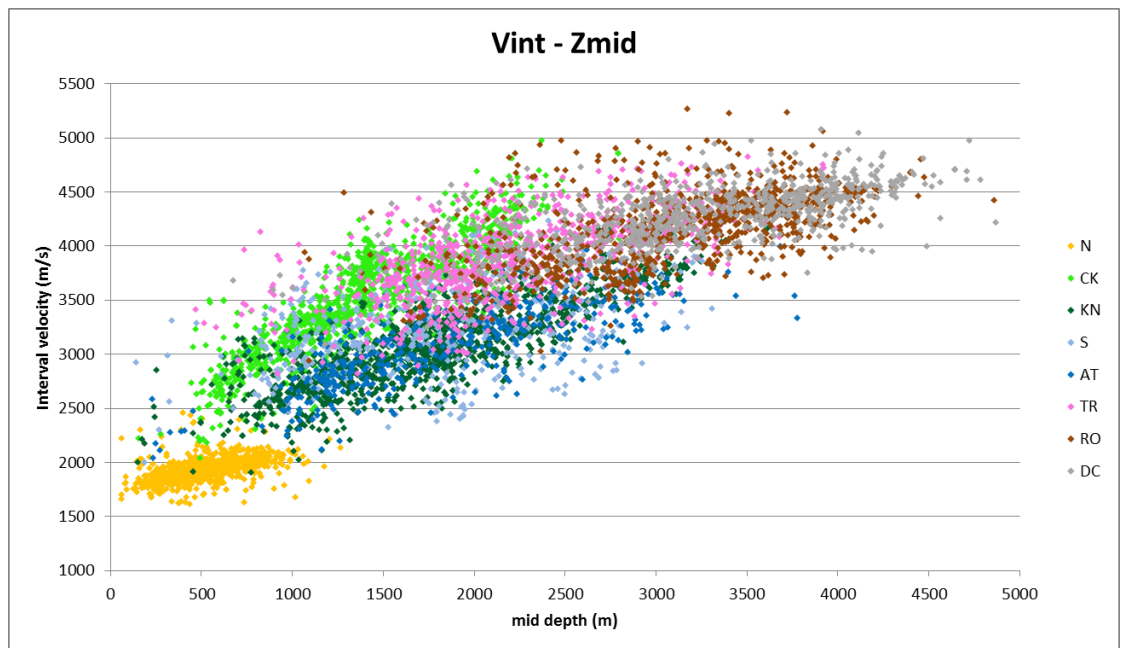


Figure 3 Interval velocity vs mid depth for each main lithostratigraphic group

Velocity curves which cover less than 25% of the drilled stratigraphic interval were discarded from the regression analysis. Also velocity curves with an interval velocity lower than 1600 m/s and higher than 6500 m/s were discarded from analysis. If the remaining dataset contained multiple velocity curves for a single well, the velocity curve with the smallest deviation with respect to the global  $V_{\text{int}} - Z_{\text{mid}}$  regression line was marked as the preferred velocity curve. After manual QC the “preferred” label was in some occasions changed to a different velocity curve. The global regression line is based on a linear least-square regression of  $V_{\text{int}}$  on  $Z_{\text{mid}}$ .

**Table 1** and Figure 4 to Figure 18 show the results of the  $V_0$  and  $k$  parameterization.

**Table 1**  $V_{int} - Z_{mid}$  regression data for the main layers of VELMOD-3

Layer	Strat	Area	# Boreholes	# velocity curves	k (s-1)	V0 (m/s)	R <sup>2</sup>
1	N	Dutch territory	1075	2544	0.284	1788	0.30
1a	NU	Dutch territory	660	1506	0.436	1761	0.32
1b	NM+NL	Dutch territory	757	1763	0.235	1779	0.32
2	CK	Dutch territory	1160	2556	0.593	2646	0.74
3	KN	Dutch territory	1225	2710	0.536	2133	0.69
3a	KNGL	Dutch territory	1128	2439	0.737	1907	0.80
3b	KNN	Dutch territory	1109	2455	0.428	2217	0.51
4	SL	Lower Saxony Basin, Central Netherlands Basin, West Netherlands Basin, Broad Fourteens Basin	458	1016	0.520	2557	0.34
4	SL	Vlieland Basin, Terschelling Basin, Step Graben	458	1016	0.520	2120	0.22
4	SL	Dutch Central Graben	458	1016	0.520	1609	0.47
5	AT	Dutch territory	419	951	0.436	2259	0.59
6	RN+RB	Dutch territory	817	1792	0.374	3046	0.38
6a	RN	Dutch territory	638	1423	0.361	3079	0.41
6b	RB	Dutch territory	937	2026	0.406	3019	0.39
8	RO	Dutch territory	901	1912	0.309	3209	0.31
9	DC	Dutch territory	780	1566	0.261	3427	0.44
9	DCG	Dutch territory	19	36	0.262	3377	0.68

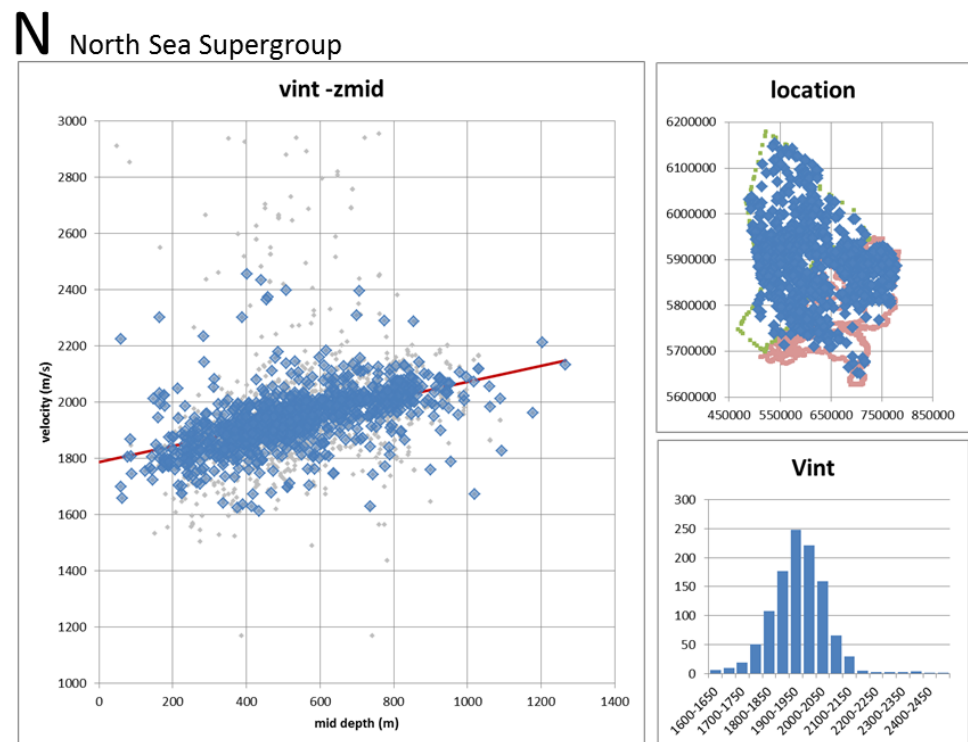


Figure 4 Interval velocity vs mid-depth (left; grey points are discarded from regression analysis), distribution (lower right) and location (upper right) of interval velocities of the North Sea Supergroup

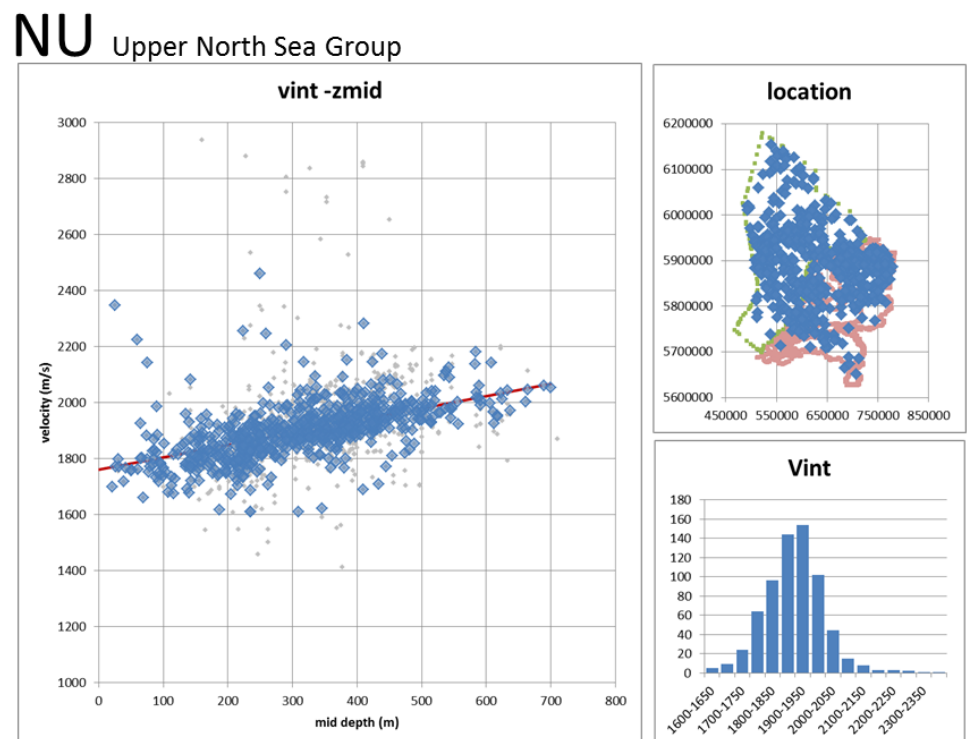


Figure 5 Interval velocity vs mid-depth (left; grey points are discarded from regression analysis), distribution (lower right) and location (upper right) of interval velocities of the Upper North Sea Group

## NM+ML Middle and Lower North Sea Group

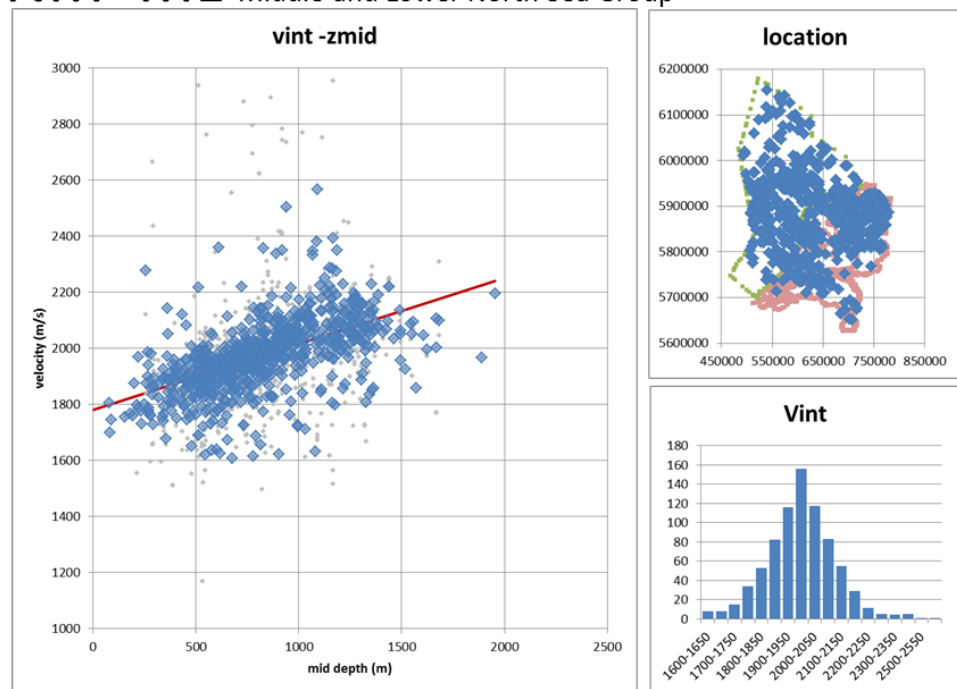


Figure 6 Interval velocity vs mid-depth (left; grey points are discarded from regression analysis), distribution (lower right) and location (upper right) of interval velocities of the Middle and Lower North Sea groups

## CK Chalk Group

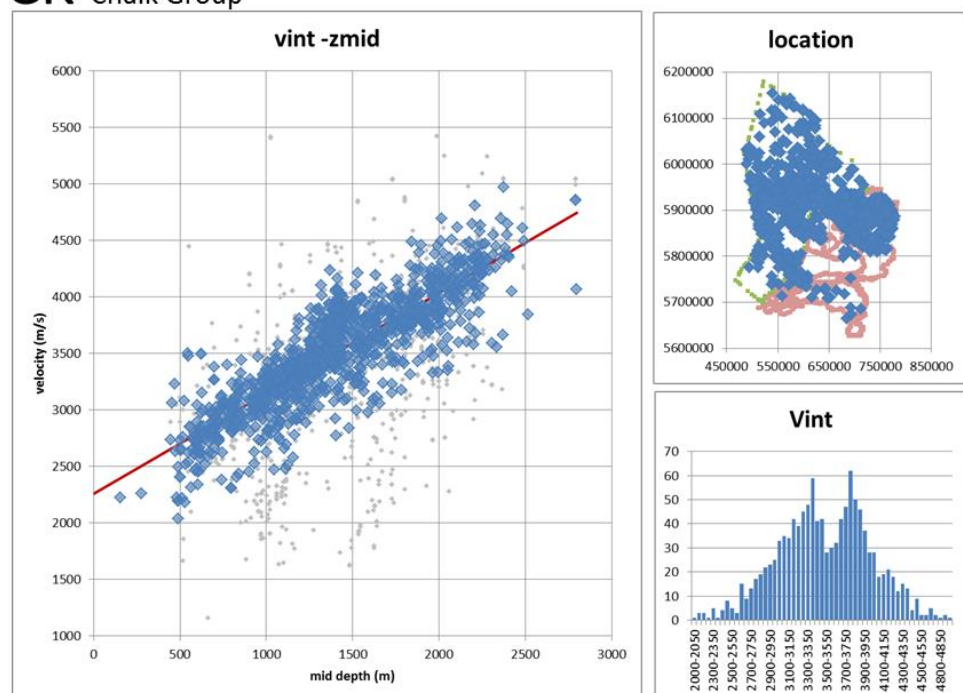


Figure 7 Interval velocity vs mid-depth (left; grey points are discarded from regression analysis), distribution (lower right) and location (upper right) of interval velocities of the Chalk Group

## KN Rijnland Group

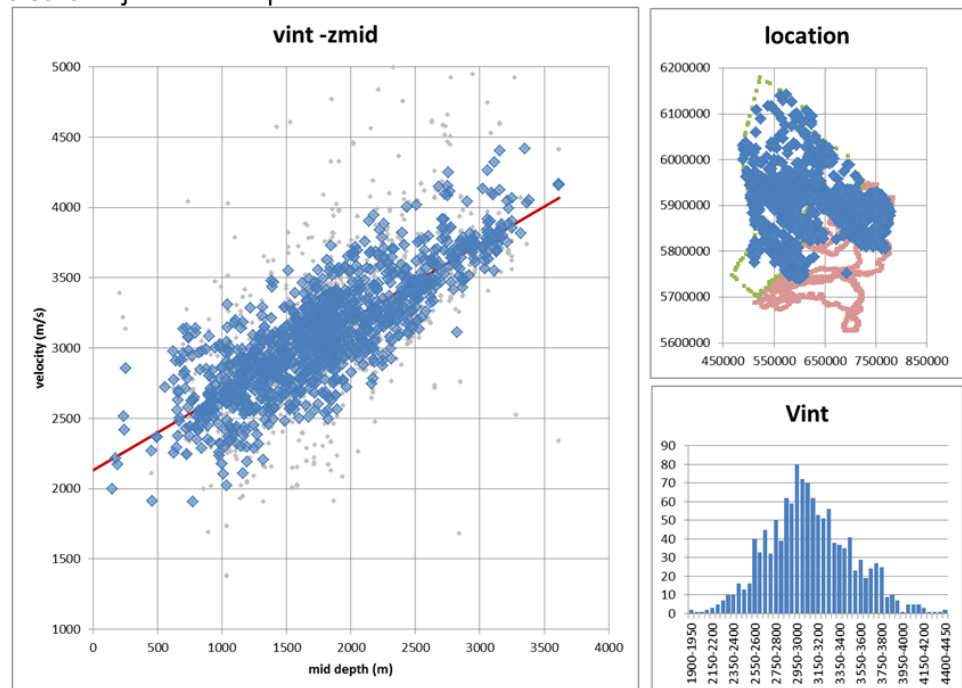


Figure 8 Interval velocity vs mid-depth (left; grey points are discarded from regression analysis), distribution (lower right) and location (upper right) of interval velocities of the Rijnland Group

## KNGL Holland Formation

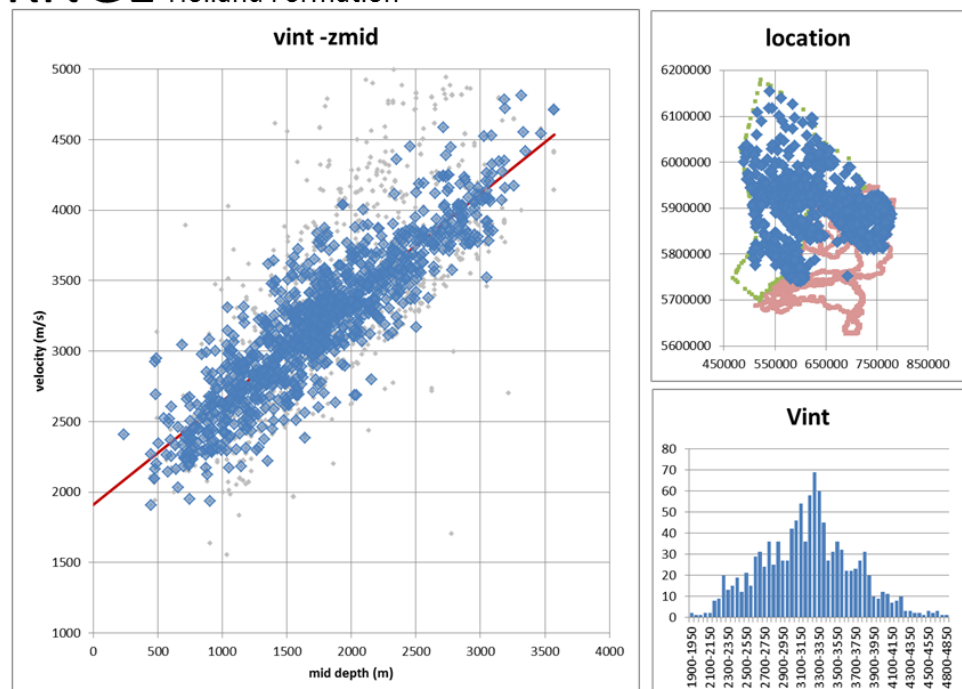


Figure 9 Interval velocity vs mid-depth (left; grey points are discarded from regression analysis), distribution (lower right) and location (upper right) of interval velocities of the Holland Formation (upper part of Rijnland Group)



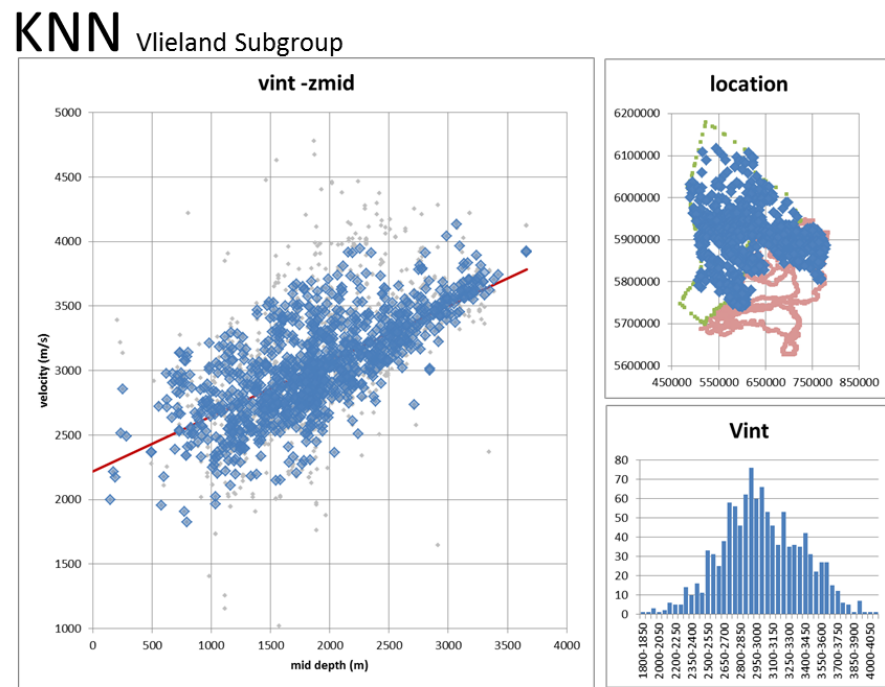


Figure 10 Interval velocity vs mid-depth (left; grey points are discarded from regression analysis), distribution (lower right) and location (upper right) of interval velocities of the Vlieland Subgroup (lower part of Rijnland Group)

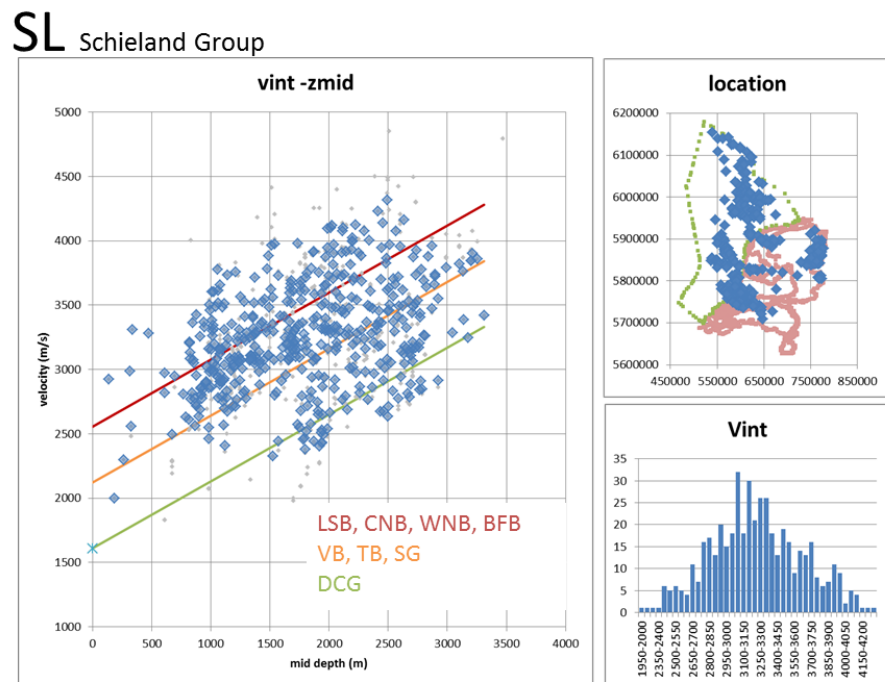


Figure 11 Interval velocity vs mid-depth (left; grey points are discarded from regression analysis), distribution (lower right) and location (upper right) of interval velocities of the Schieland Group. Regression subdivide in basin clusters LSB: Lower Saxony Basin, CNB: Central Netherlands Basin, WNB: West Netherlands Basin, BFB: Broad Fourteens Basin, VB: Vlieland Basin, TB: Terschelling Basin, SG: Step Graben, DCG: Dutch Central Graben.



## AT Altena Group

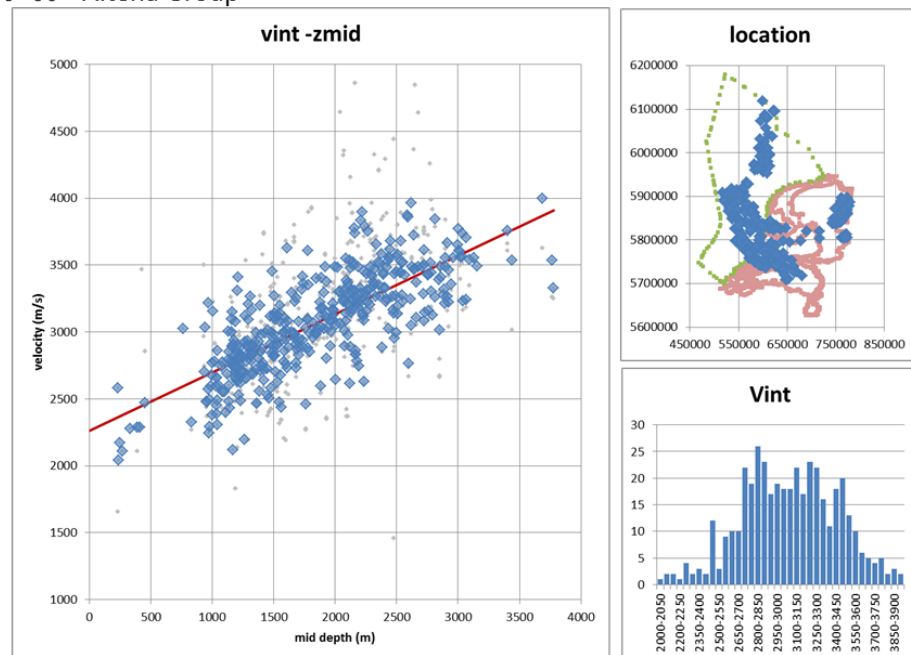


Figure 12 Interval velocity vs mid-depth (left; grey points are discarded from regression analysis), distribution (lower right) and location (upper right) of interval velocities of the Altena Group.

## RN+RB Upper and Lower Germanic Trias Group

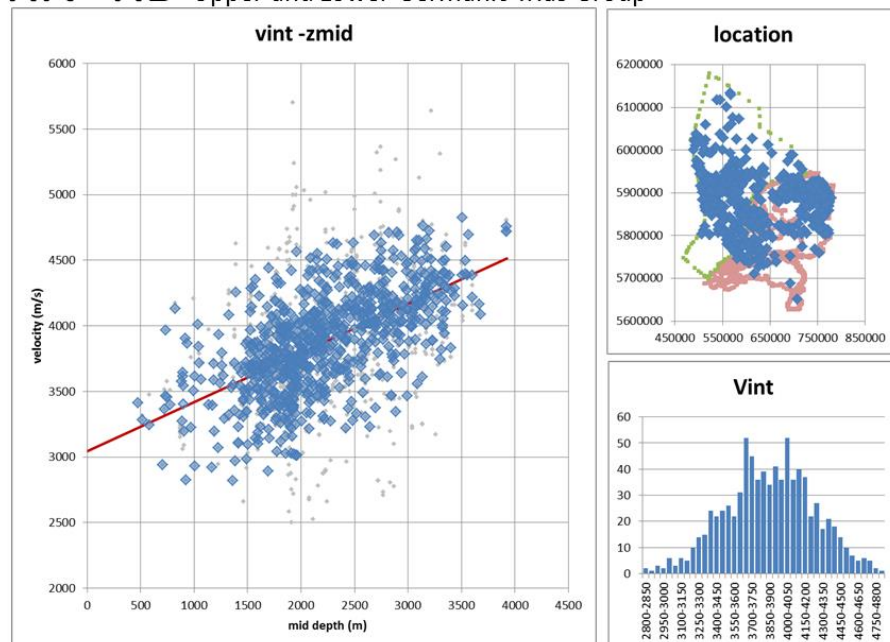


Figure 13 Interval velocity vs mid-depth (left; grey points are discarded from regression analysis), distribution (lower right) and location (upper right) of interval velocities of the Upper and Lower Germanic Trias groups.

## RN Upper Germanic Trias Group

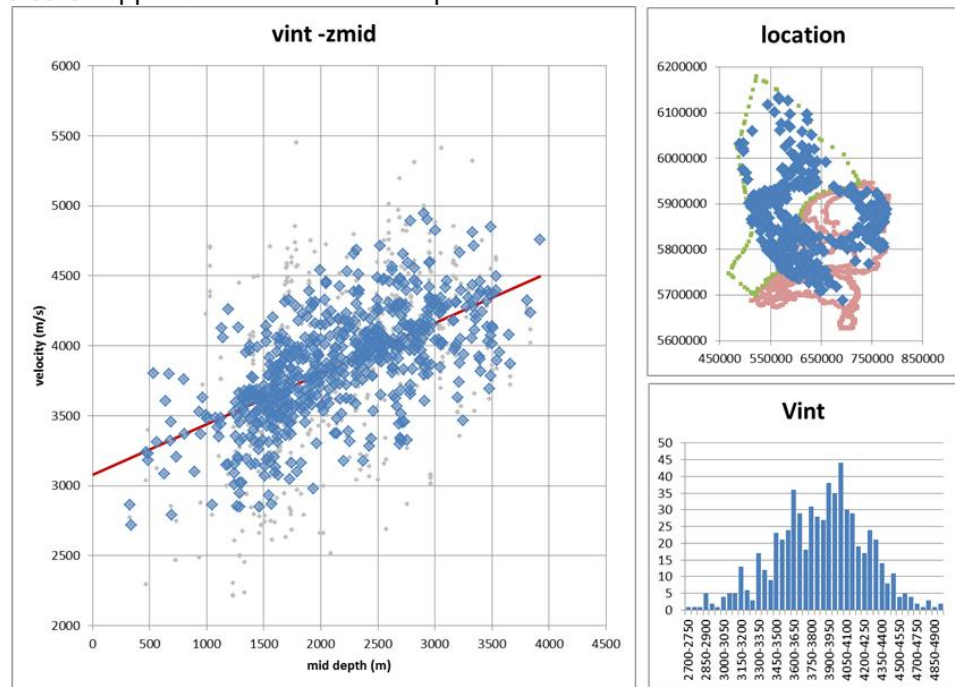


Figure 14 Interval velocity vs mid-depth (left; grey points are discarded from regression analysis), distribution (lower right) and location (upper right) of interval velocities of the Upper Germanic Trias Group.

## RB Lower Germanic Trias Group

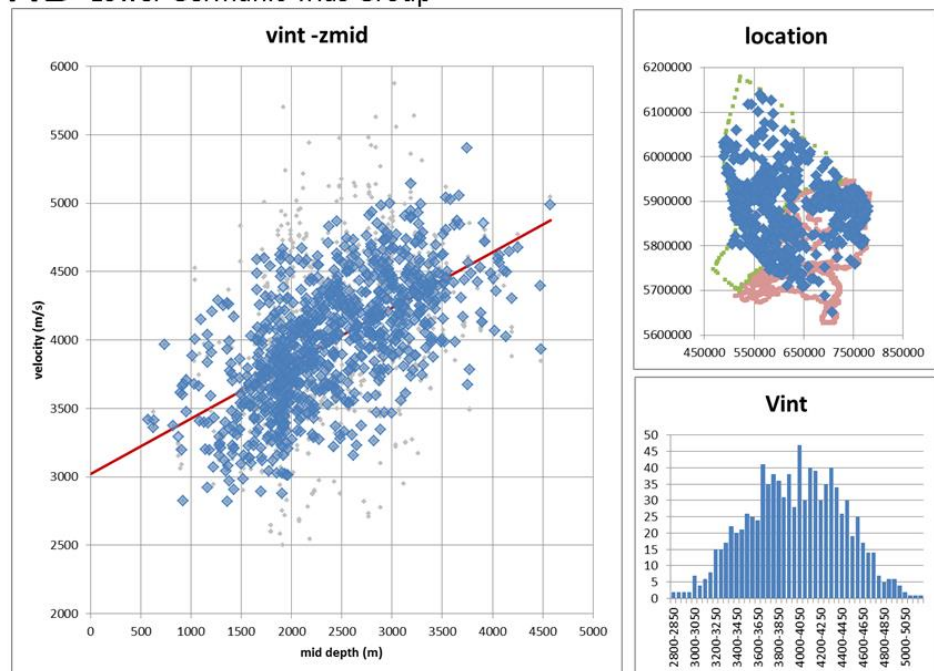


Figure 15 Interval velocity vs mid-depth (left; grey points are discarded from regression analysis), distribution (lower right) and location (upper right) of interval velocities of the Lower Germanic Trias Group.

## RO Upper Rotliegend Group

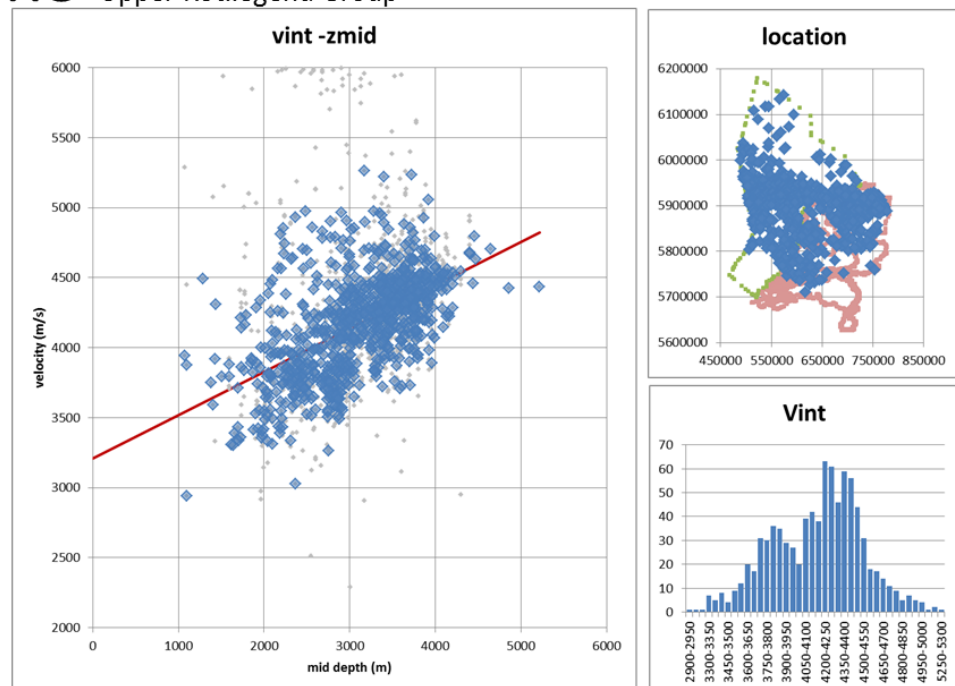


Figure 16 Interval velocity vs mid-depth (left; grey points are discarded from regression analysis), distribution (lower right) and location (upper right) of interval velocities of the Upper Rotliegend Group.

## DC Limburg Group (Westphalian)

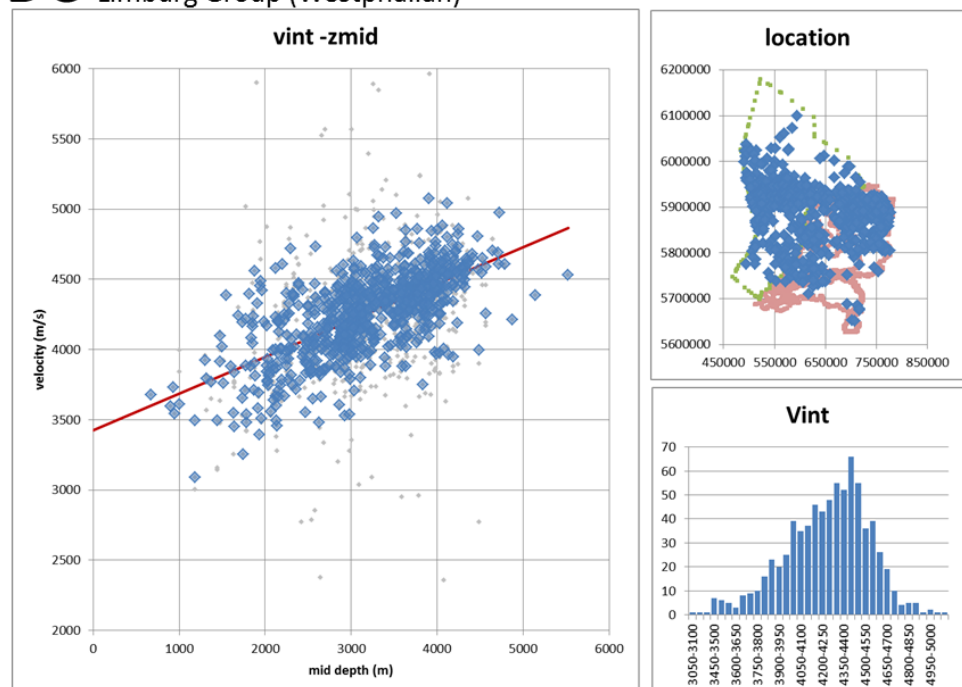


Figure 17 Interval velocity vs mid-depth (left; grey points are discarded from regression analysis), distribution (lower right) and location (upper right) of interval velocities of the Limburg Group, the vast majority only penetrates the upper part of Westphalian aged stata.

## DCG Geul Subgroup (Namurian)

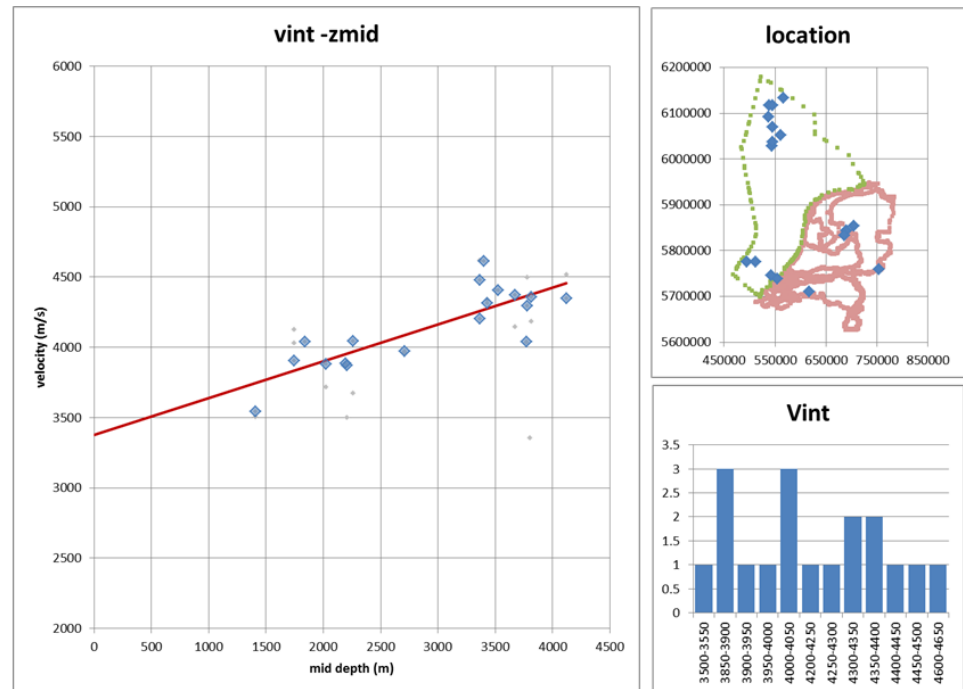


Figure 18 Interval velocity vs mid-depth (left; grey points are discarded from regression analysis), distribution (lower right) and location (upper right) of interval velocities of the Geul Subgroup (Namurian age).

On the basis of the global parameterization of  $k$ , the local  $V_0$  at the location of well is estimated by 2 different methods:

“*Local  $V_0_{basefit}$* ” calibration based on the total vertical traveltime  $\Delta T$  of the sonic data (Japsen, 1993) using the following calibration formula:

$$V_0 = \frac{k (Z_b - Z_t e^{k\Delta T})}{e^{k\Delta T} - 1} \quad (\text{eq. 2})$$

“*Local  $V_0_{rms}$* ” calibration based on the least square error of all velocity data points per well with regard to the velocities derived from the  $V_0$ - $k$  model.

An example of the difference between the two methods is visualized in Figure 19. Although the *Local  $V_0_{basefit}$*  calibration results a zero depth error at the base of the stratigraphic interval, the *Local  $V_0_{rms}$*  calibration gives the smallest average depth error over the complete stratigraphic interval.

VELMOD-3 is large scale regional velocity model and will primary be used for seismic time-depth conversion, therefore  $V_0$  results based on the *Local  $V_0_{basefit}$*  calibration were used for the construction of regional  $V_0$  distribution maps. Results of both methods are reported (see Appendix B).

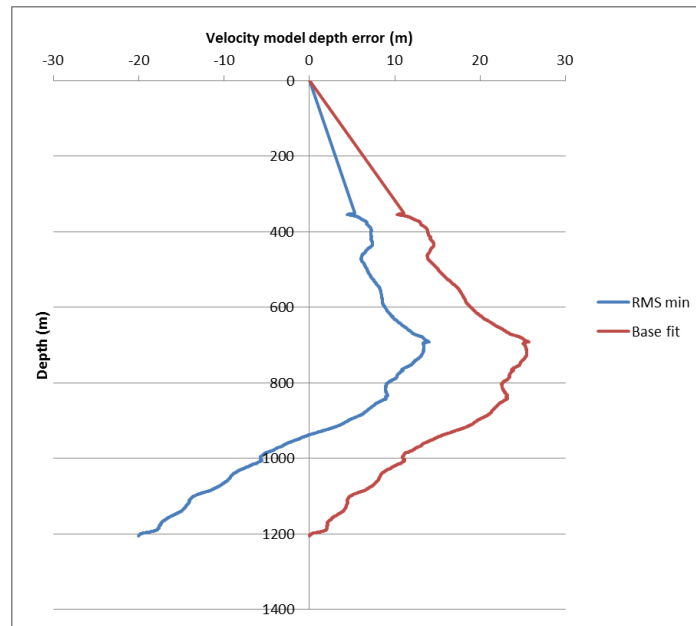


Figure 19 Depth error of different local V0 model estimates at well KDK-01. Shown depth error is the difference between modelled velocity and instantaneous velocity from sonic log.

### 3.4 Zechstein and other groups

The lithology of the Zechstein in general consist of anhydrite, halite, and/or carbonate. The lithological composition of the interval is the most dominant factor for the interval velocity. The influence of compaction on the interval velocity is considered very minor.

Zechstein interval velocity is modelled based on velocity - thickness (or  $\Delta T$ ) relation from wells (Figure 20). In general, layers with limited thickness show the relative high abundance of high velocity carbonate layers (Kombrink et al, 2012).

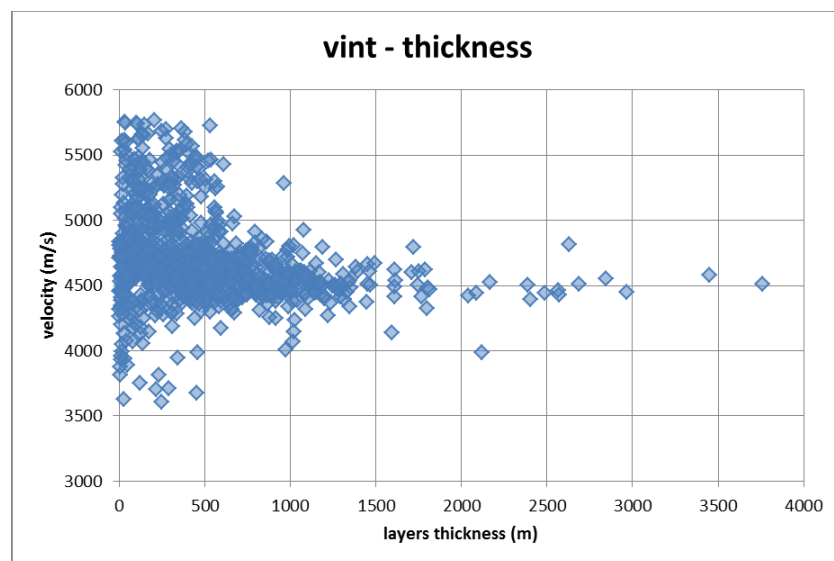


Figure 20 Thickness versus interval velocity of the Zechstein layer.

Interval velocities of other Paleozoic lithostratigraphic groups were processed. Because of the limited amount of data, no velocity depth trend was derived for

these intervals. For completeness the data points are shown in Figure 21 to Figure 25 and a data overview is given in Table 2.

Table 2 Overview of data availability of non-compacting layers and/or layers with a very limited dataset

Strat	Area	# Boreholes	# velocity curves
ZE	Dutch territory	1063	2270
RV	Dutch territory	11	18
CL	Dutch territory	7	11
CF	Dutch territory	8	17
OB+OR	Dutch territory	10	15

## ZE Zechstein Group

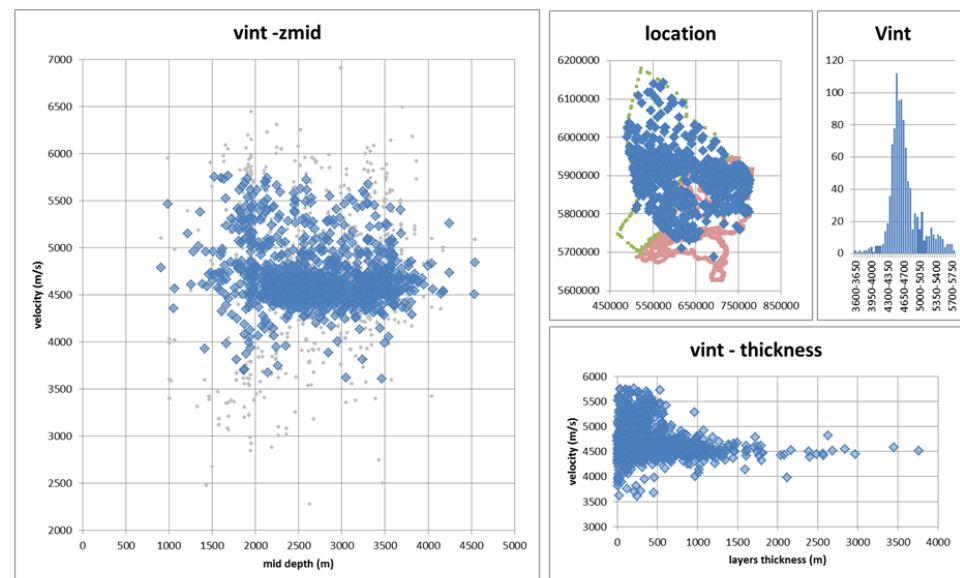


Figure 21 Interval velocity vs mid-depth (left; grey points are duplicates), distribution & location (upper right) of interval velocities and interval velocity vs thickness (lower right) of the Zechstein Group.

## RV Lower Rotliegend Group

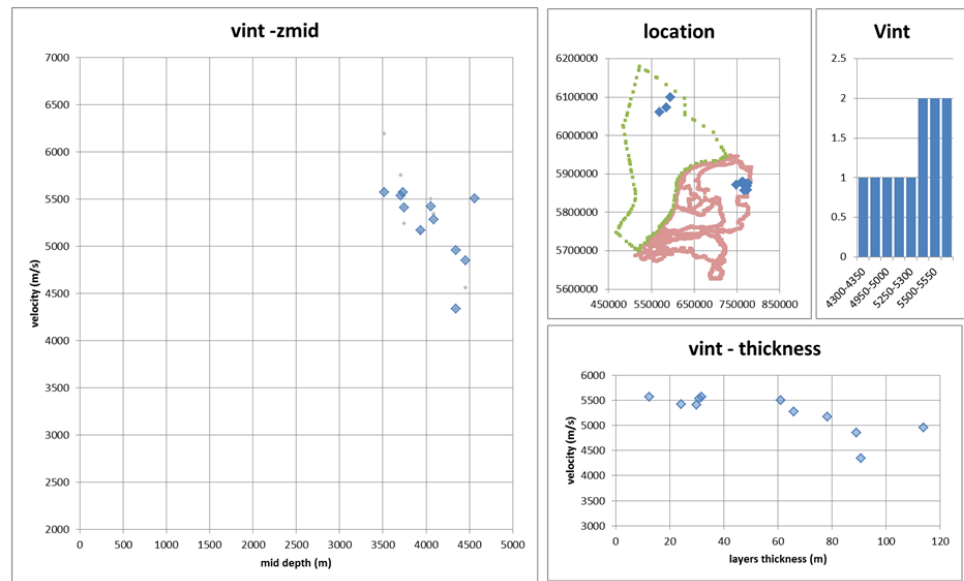


Figure 22 Interval velocity vs mid-depth (left; grey points are duplicates), distribution & location (upper right) of interval velocities and interval velocity vs thickness (lower right) of the Lower Rotliegend Group.

## CL Carboniferous Limestone Group (Dinantian)

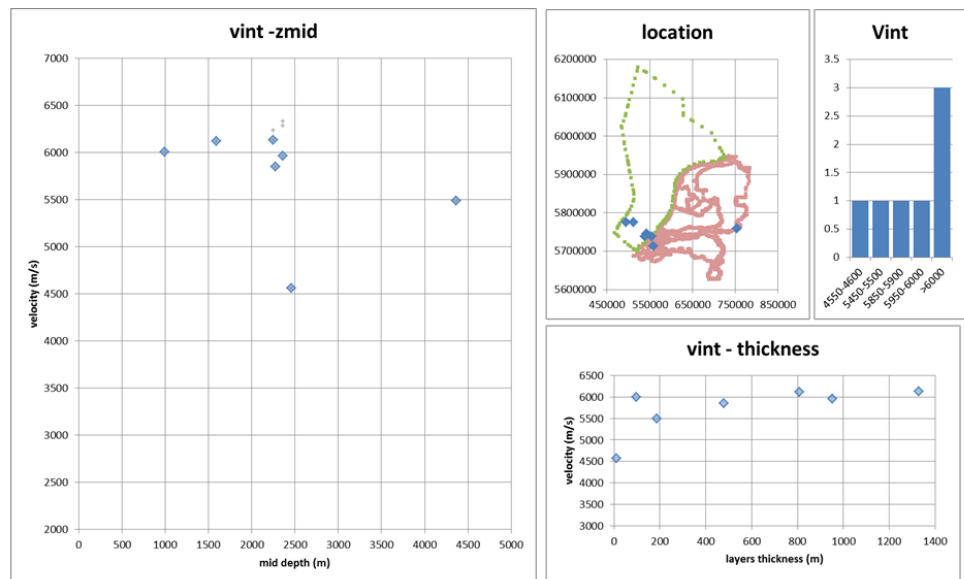


Figure 23 Interval velocity vs mid-depth (left; grey points are duplicates), distribution & location (upper right) of interval velocities and interval velocity vs thickness (lower right) of the Carboniferous Limestone Group (Dinantian age)

## CF Farne Group (Dinantian)

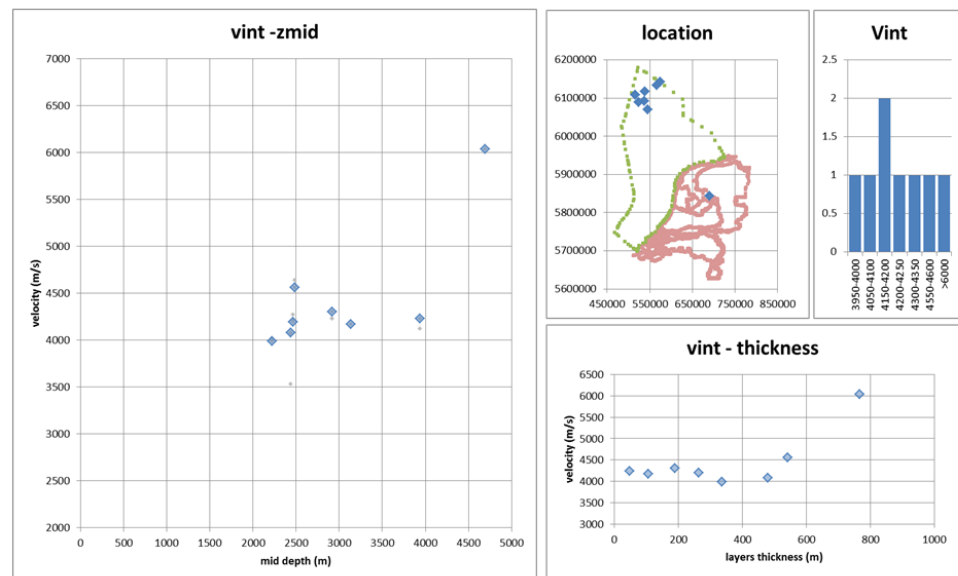


Figure 24 Interval velocity vs mid-depth (left; grey points are duplicates), distribution & location (upper right) of interval velocities and interval velocity vs thickness (lower right) of the Farne Group (dinantian age, clastic sediments).

## OB+OR Banjaard and Old Red Group (Devonian and older)

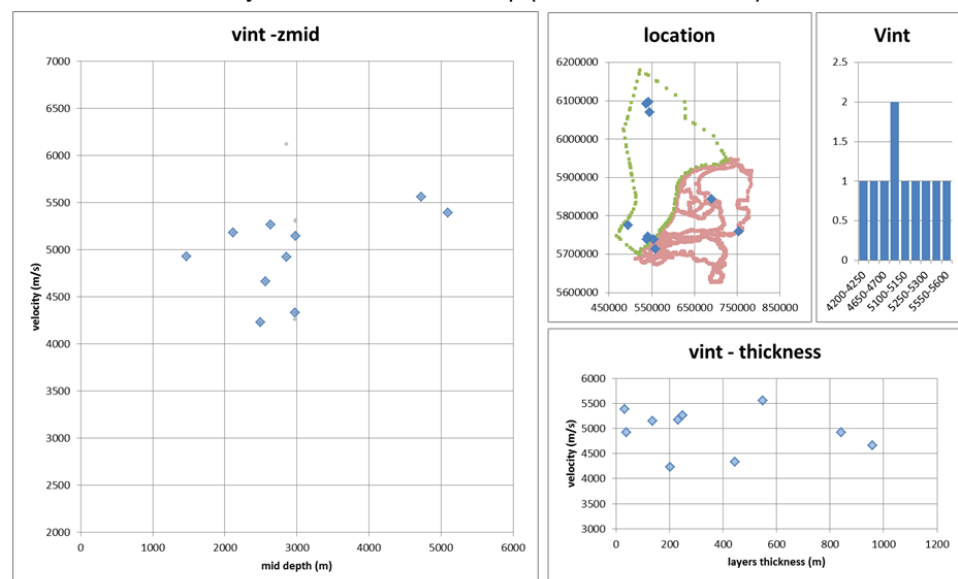


Figure 25 Interval velocity vs mid-depth (left; grey points are duplicates), distribution & location (upper right) of interval velocities and interval velocity vs thickness (lower right) of the Banjaard and Old Red Group. (aged Devonian and older)



## 4 Results

### 4.1 Spatial data analysis

Minor attention was given to spatial analysis and QC of the borehole derived  $V_{\text{int}}$  and  $V_0$  parameters. Although duplicate located values for all velocity intervals were removed, only data points of the onshore part of the North Sea Groups and the Chalk Group were subject to residual analysis with regard to depth conversion with the resulting  $V_{\text{int}}$  and  $V_0$  grids of this project. This iterative process led to the removal of a number of data point with unreliable velocity values.

Gridding of the  $V_{\text{int}}$  and  $V_0$  data points was conducted with Petrel modelling software. The grid cell size is 1000m x 1000m. Simple kriging was applied. A spherical variogram model was used with a relative nugget of 10% of the total variance. Variogram ranges were obtained through exploratory data analysis (Isatis statistic software). Used variogram ranges are listed in Table 3.

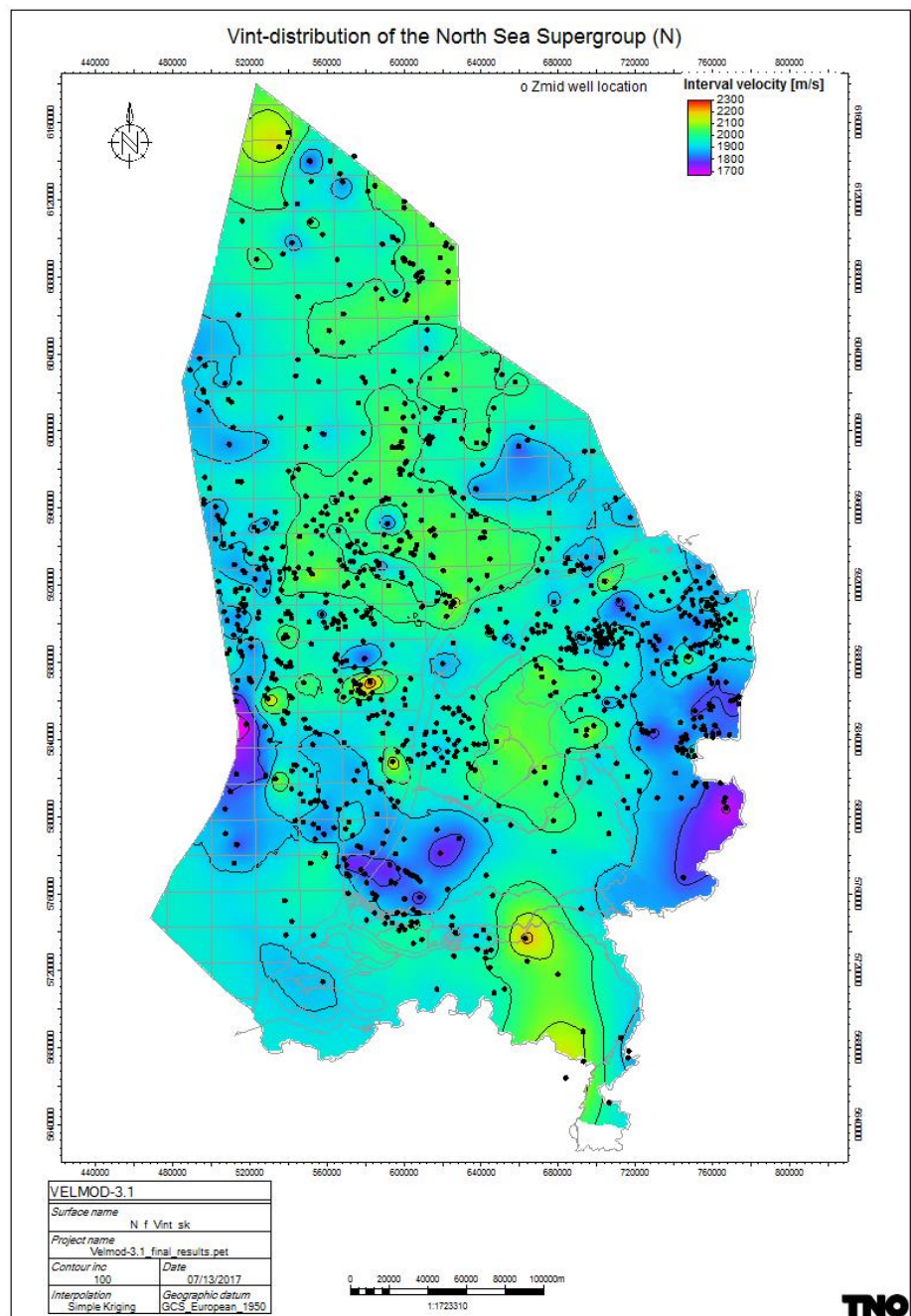
Table 3. Derive variogram ranges

Strat interval	range $V_{\text{int}}$ [km]	range $V_0$ [km]
N	60	25
NU	40	25
NM+NL	100	35
CK	75	45
KN	60	60
KNGL	77	32
KNN	50	50
SL	45	54
AT	55	50
RN+RB	50	55
RN	50	45
RB	50	60
RO	55	60
DC	50	20

### 4.2 Regional $V_{\text{int}}$ distribution maps

Resulting  $V_{\text{int}}$  distribution grids are shown in Figure 26 to 40. The related kriging standard deviation maps are shown in appendix C.

In general interval velocities increase with depth due to compaction of the rocks. To make a better estimation of  $V_{\text{int}}$  between the known data points, it is useful to take depth variations into account, especially in areas with low spatial data density. Therefore also  $V_{\text{int}}$  distribution grids are generated that are the result of co-kriging  $V_{\text{int}}$  with the interpreted seismic time grids (twt) as a secondary input variable. A correlation coefficient of 65% was assigned. These results are shown in Appendix C.

Figure 26  $V_{int}$  distribution of the North Sea Supergroup

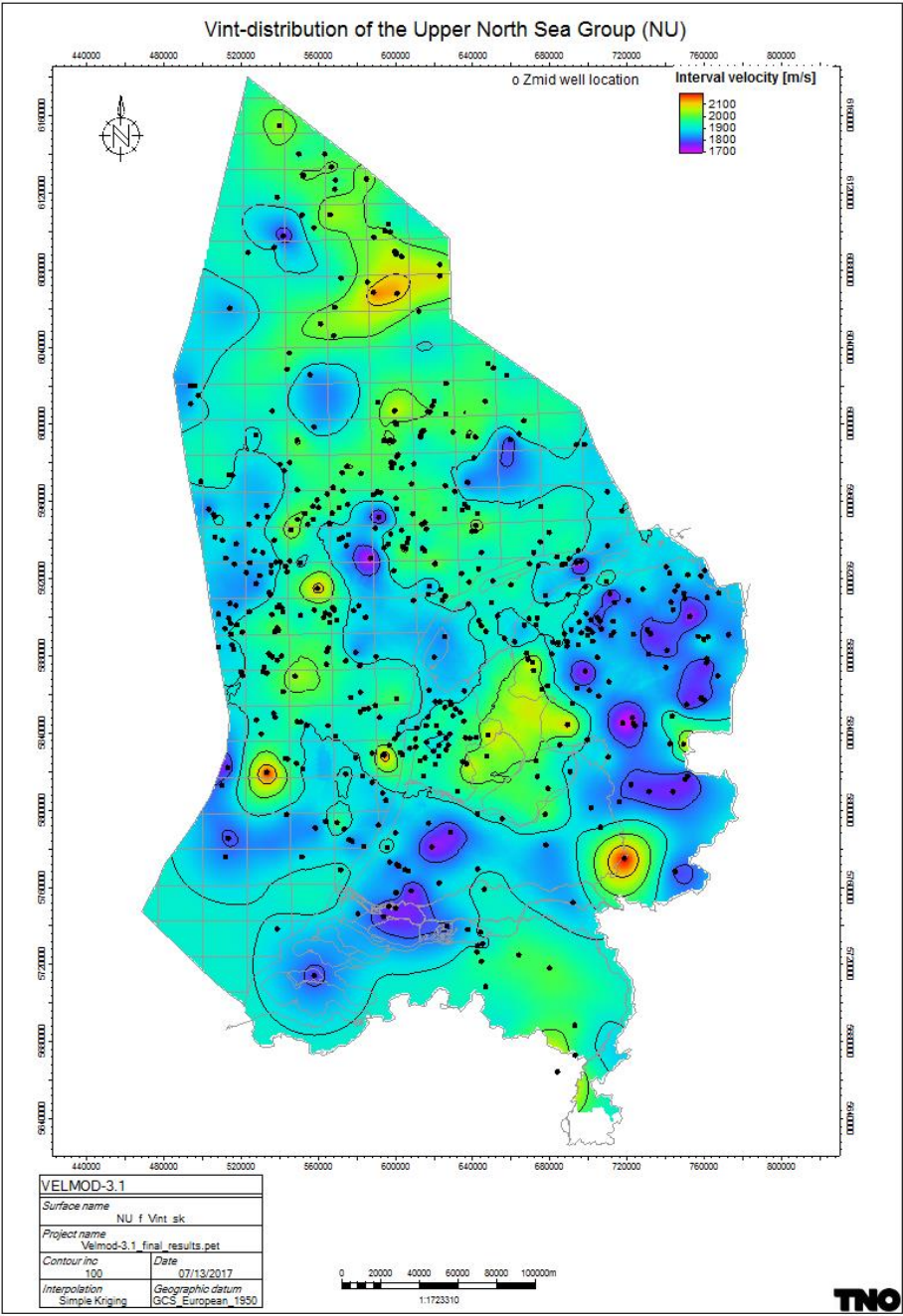
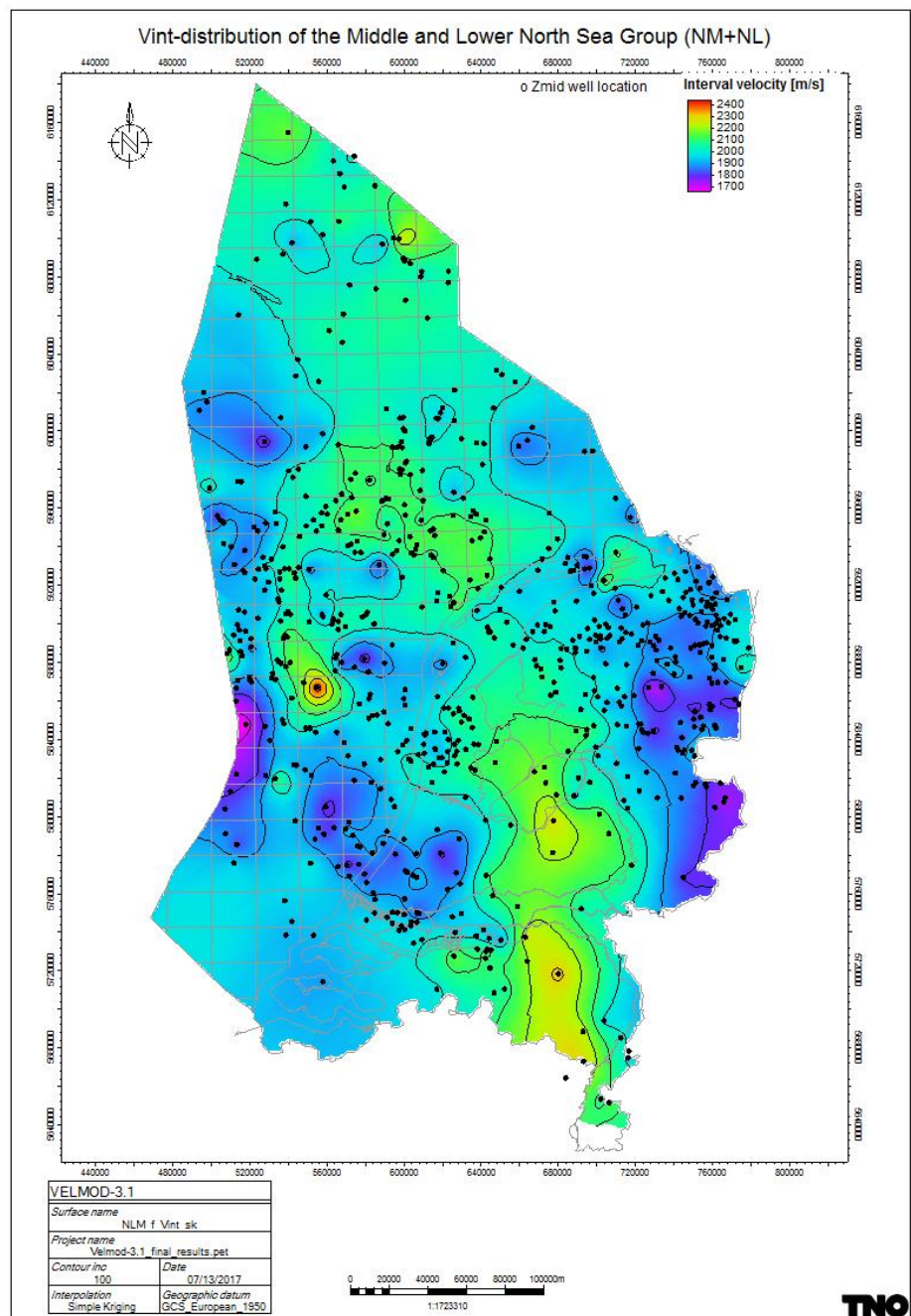


Figure 27  $V_{int}$  distribution of the Upper North Sea Group

Figure 28  $V_{int}$  distribution of the Middle and Lower North Sea groups

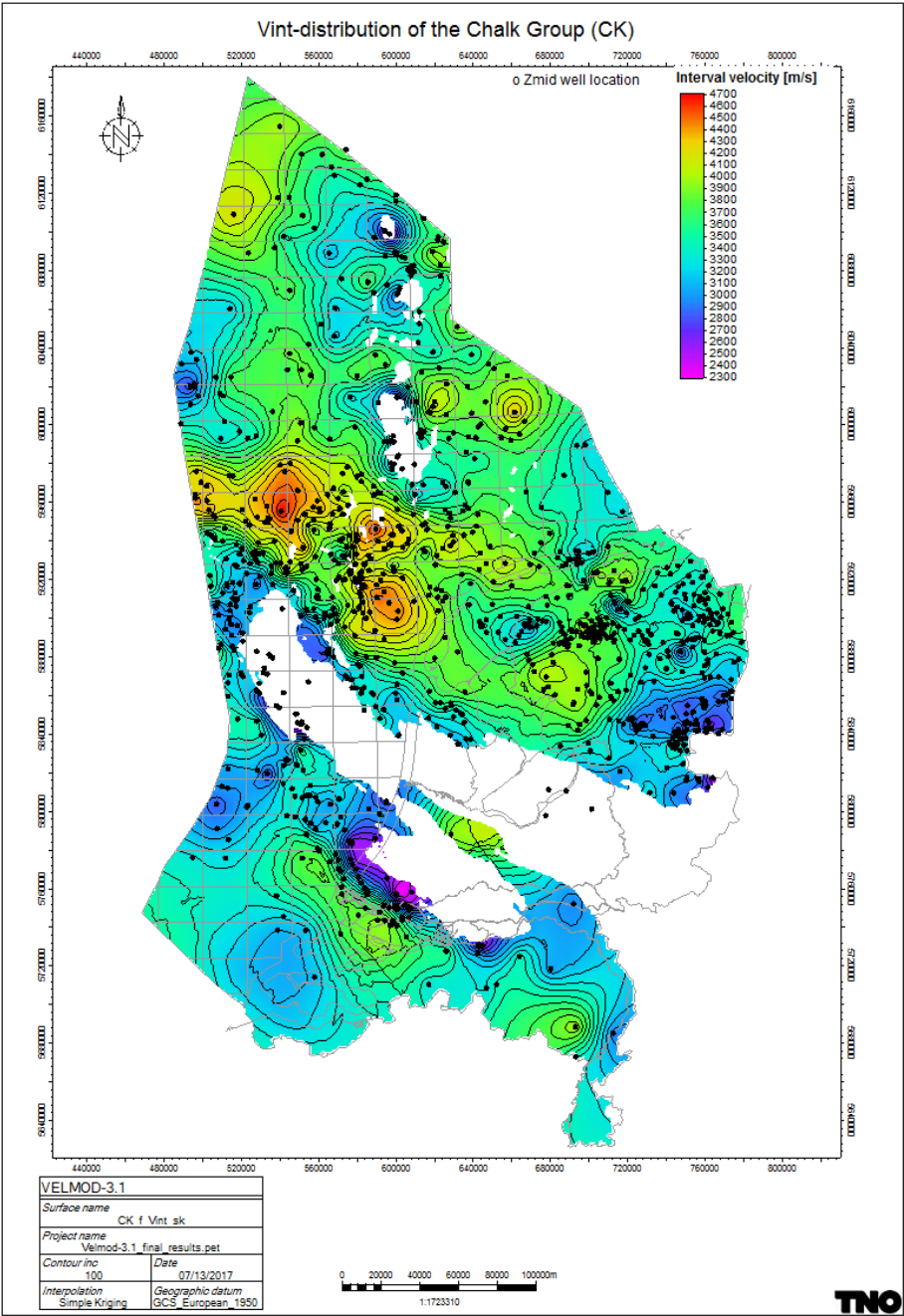
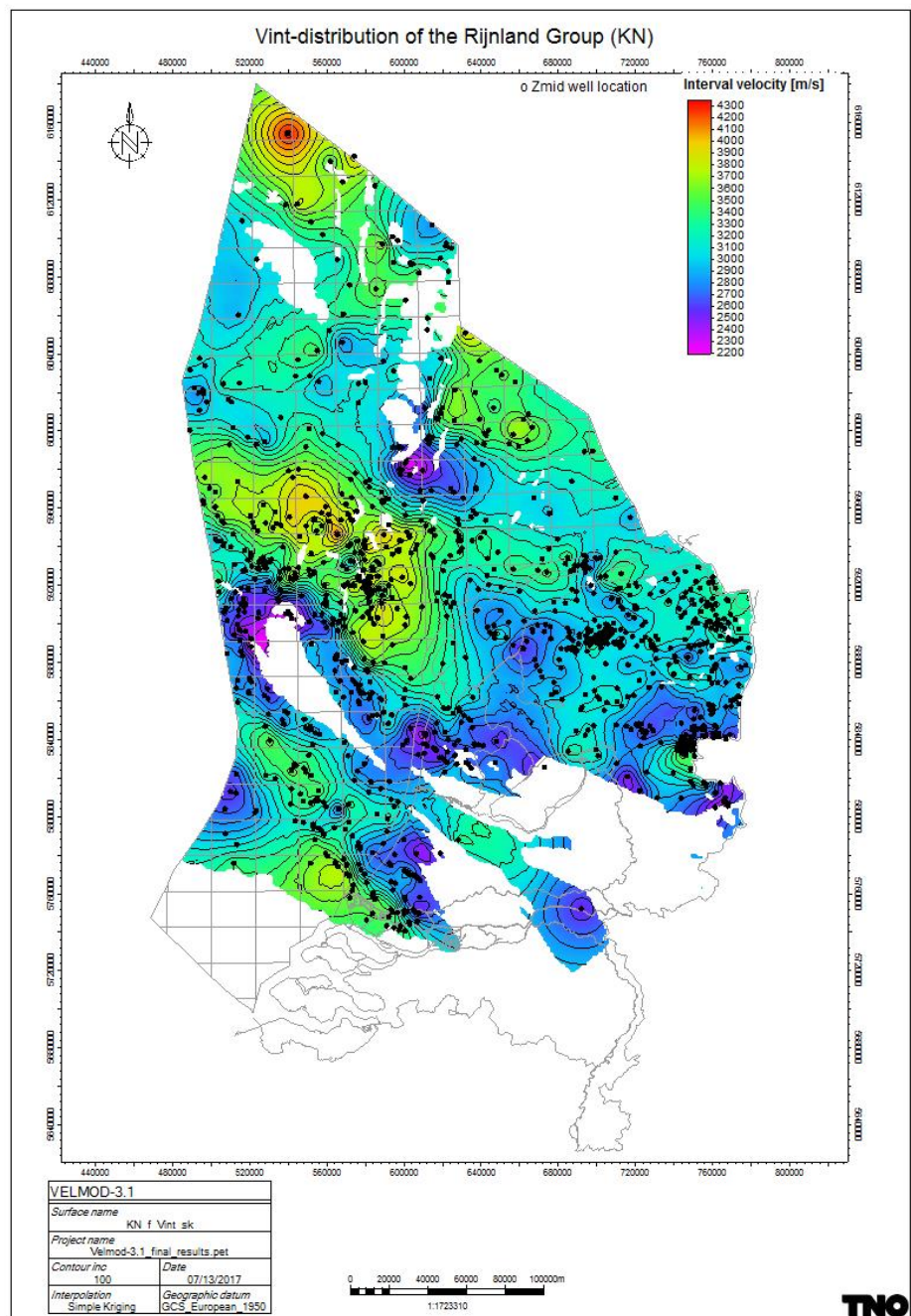
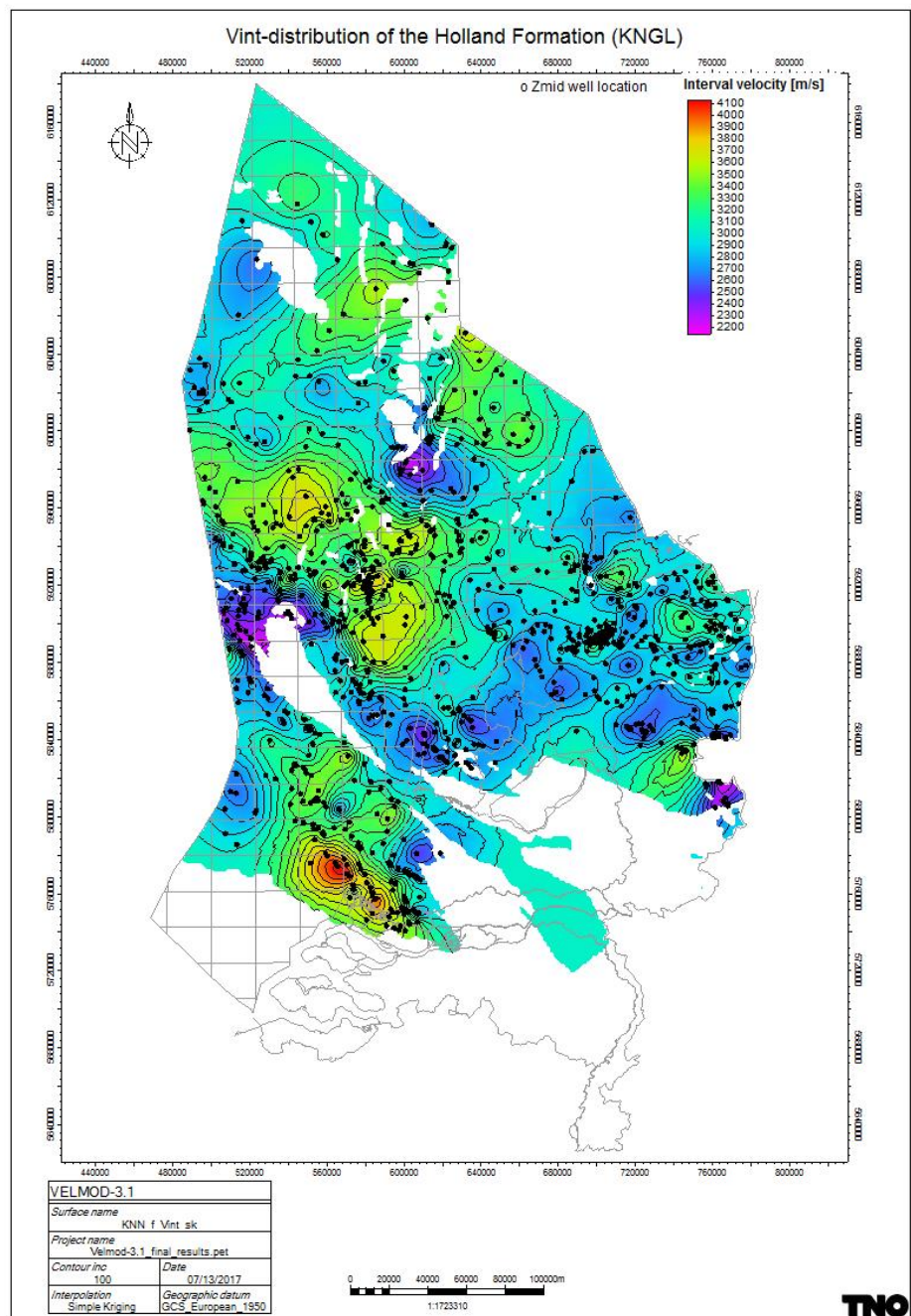
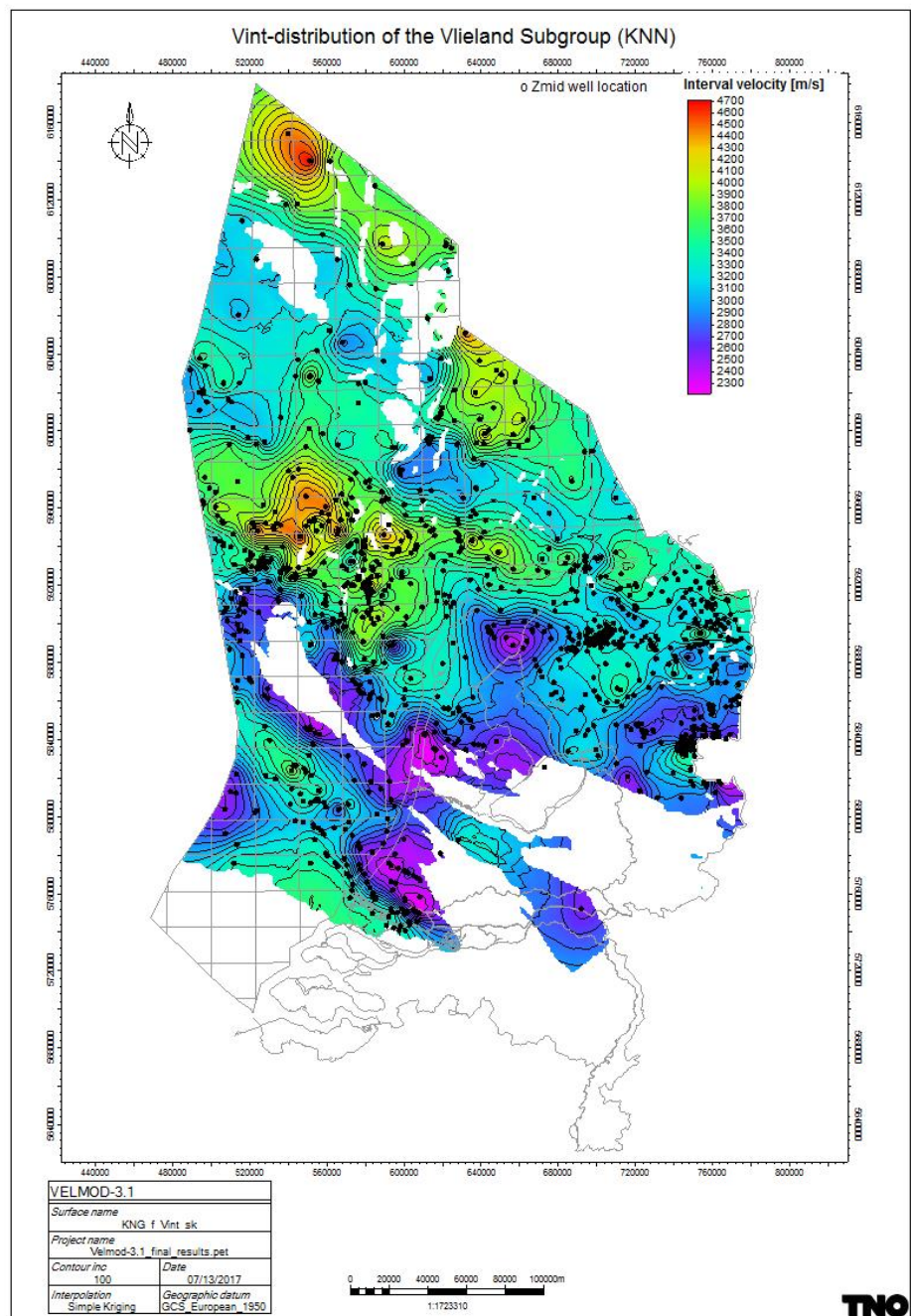


Figure 29  $V_{int}$  distribution of the Chalk Group



Figure 30  $V_{int}$  distribution of the Rijnland Group

Figure 31  $V_{int}$  distribution of the Holland Formation

Figure 32  $V_{int}$  distribution of the Vlieland Subgroup



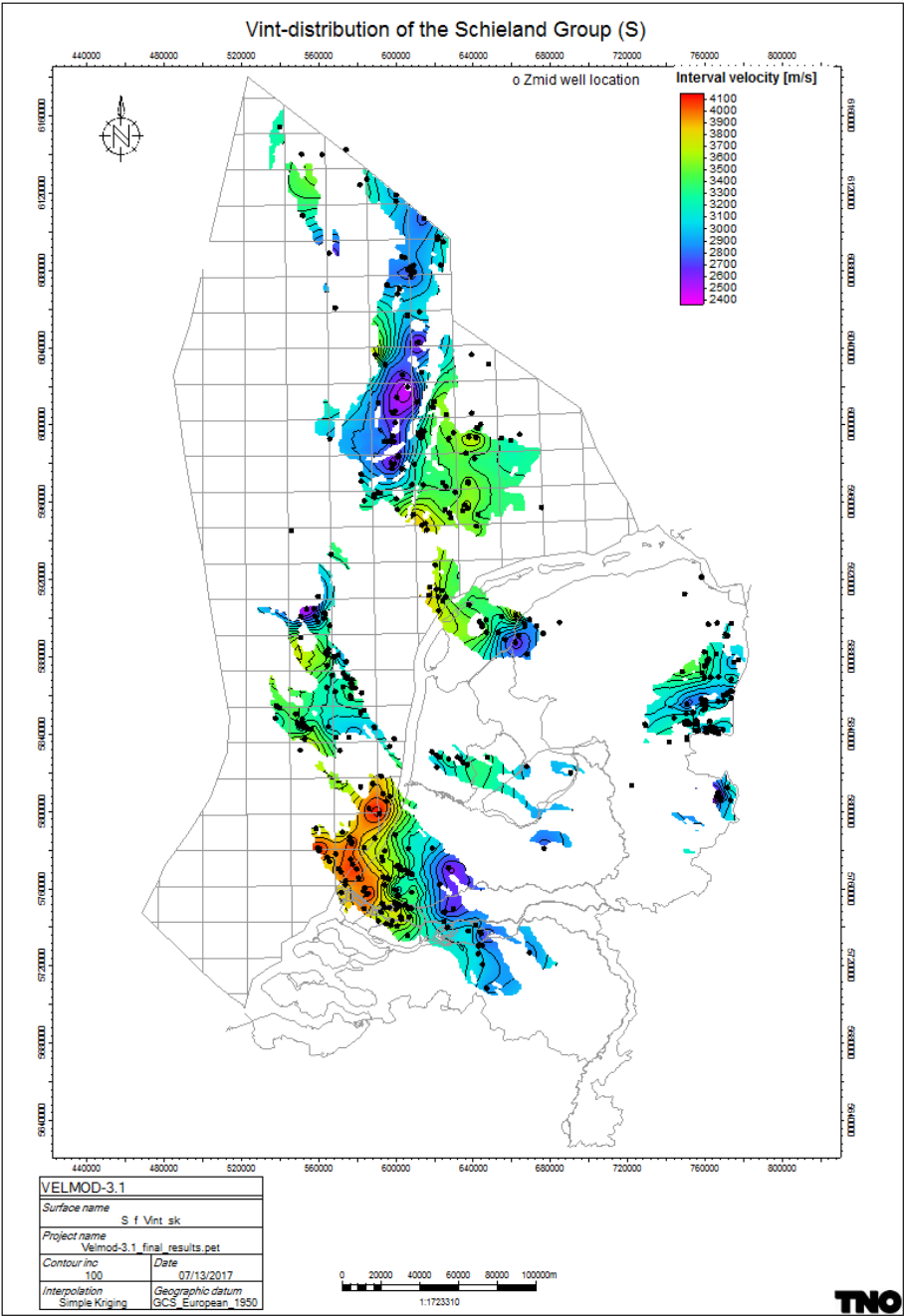
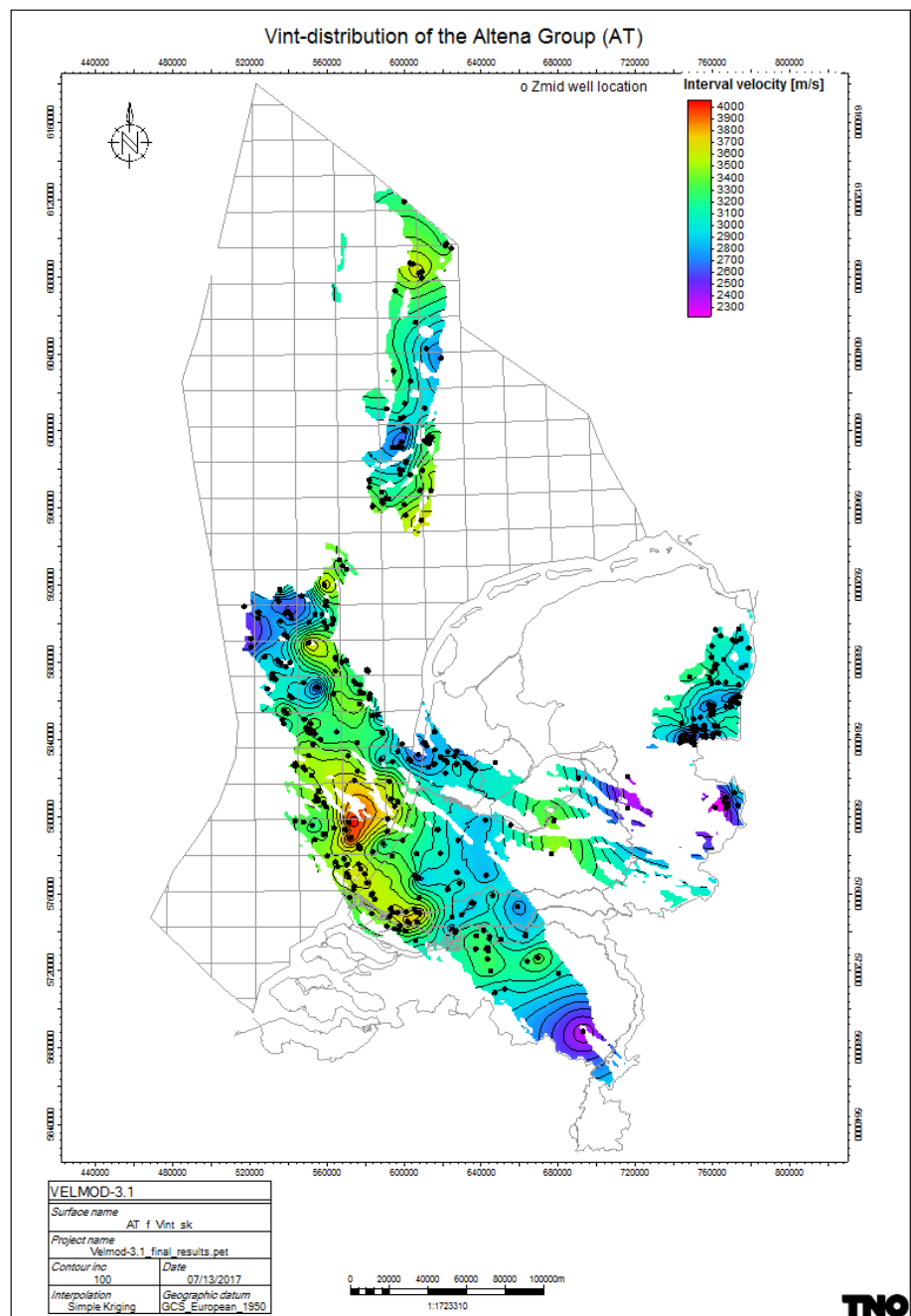
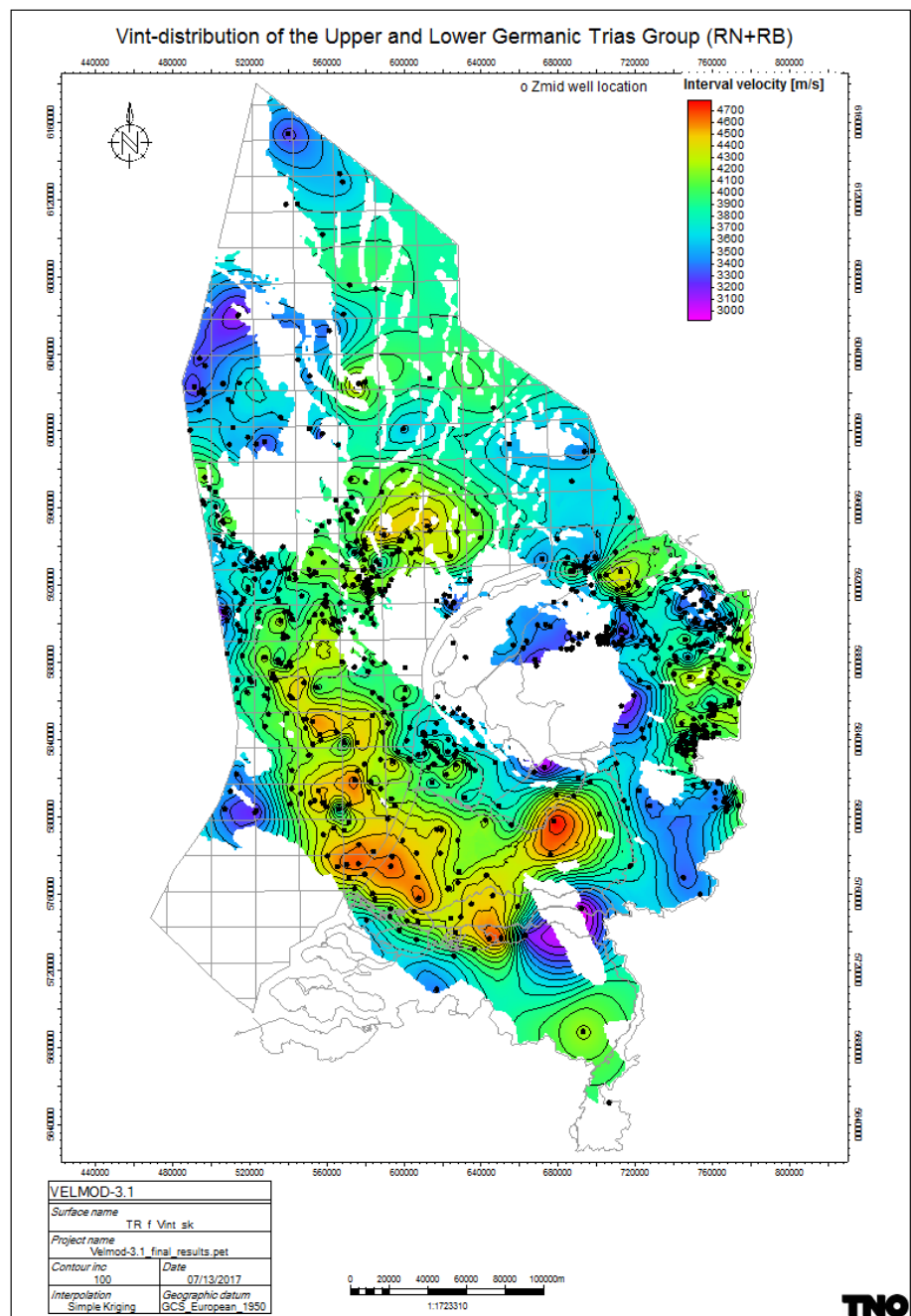
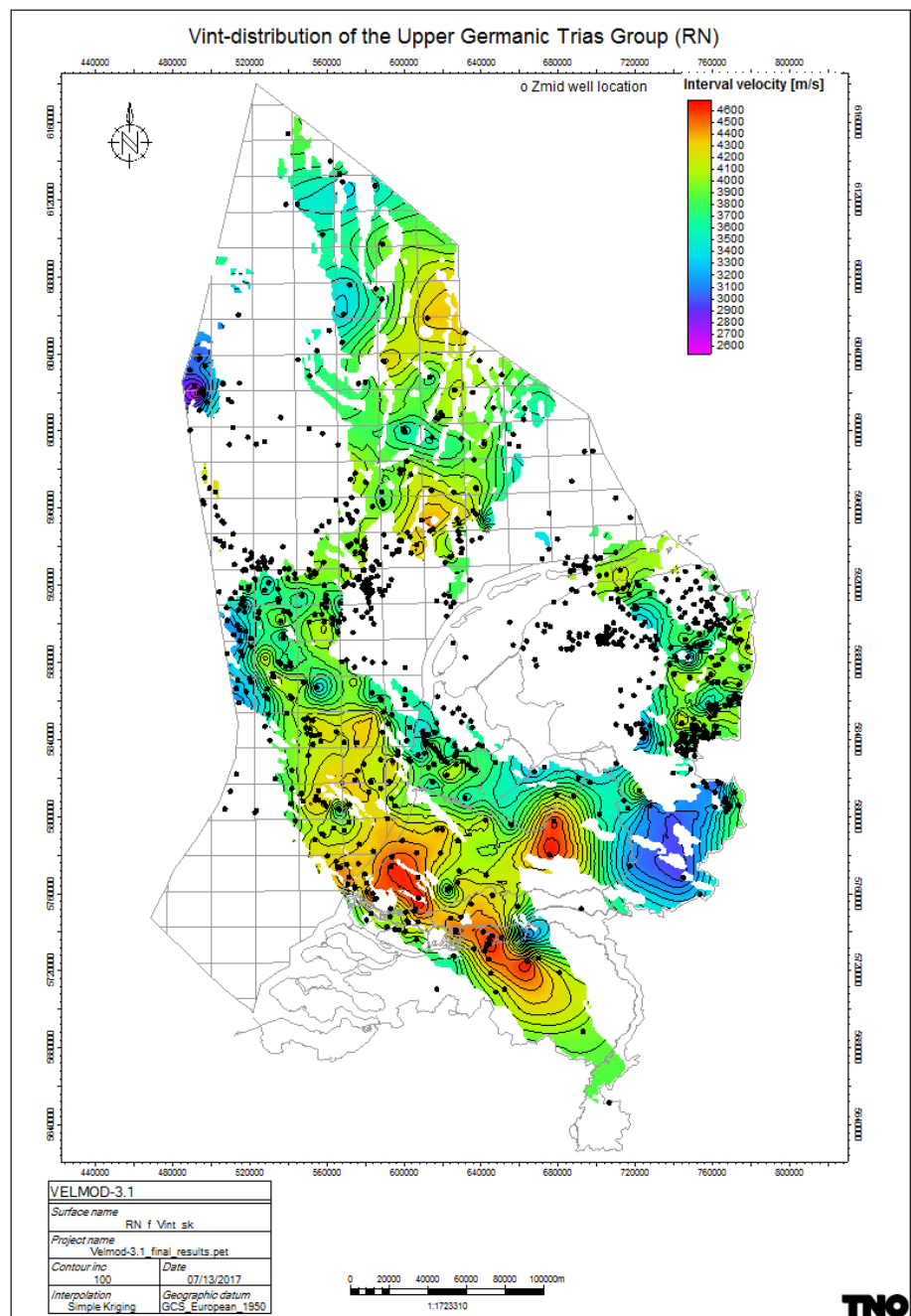


Figure 33  $V_{int}$  distribution of the Schieland Group

Figure 34  $V_{int}$  distribution of the Altena Group

Figure 35  $V_{int}$  distribution of the Upper and Lower Germanic Trias groups

Figure 36  $V_{int}$  distribution of the Upper Germanic Trias Group

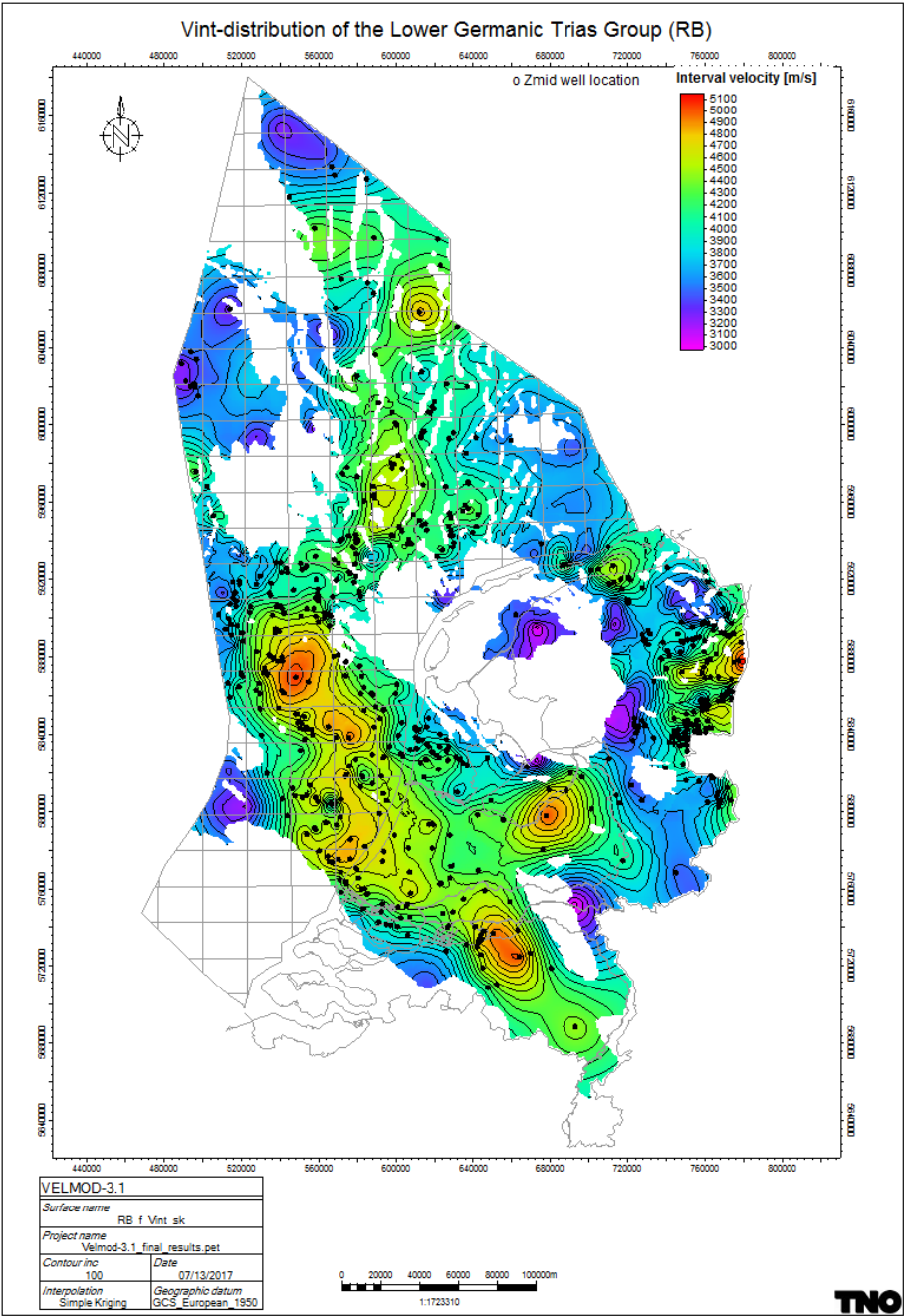
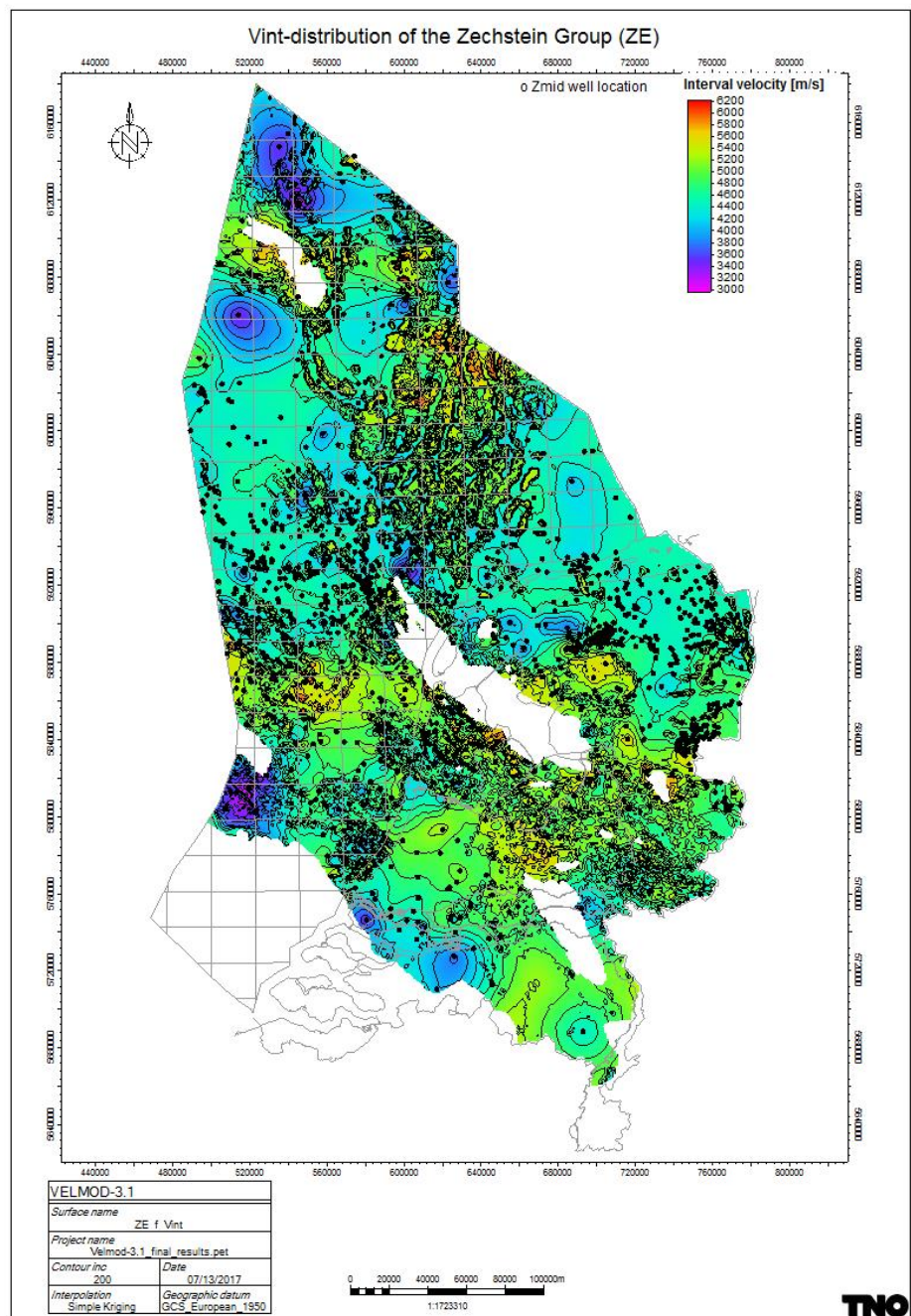
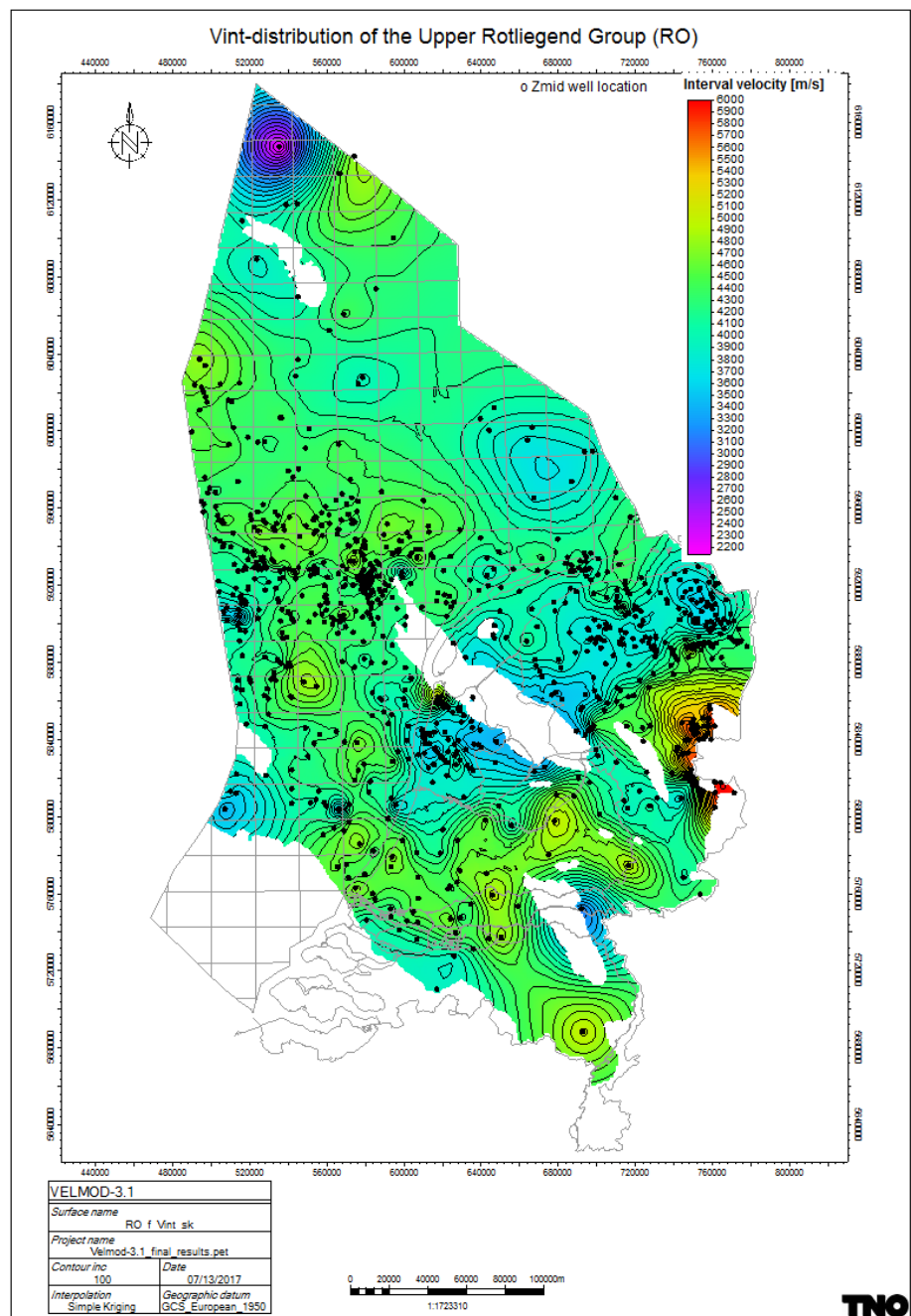
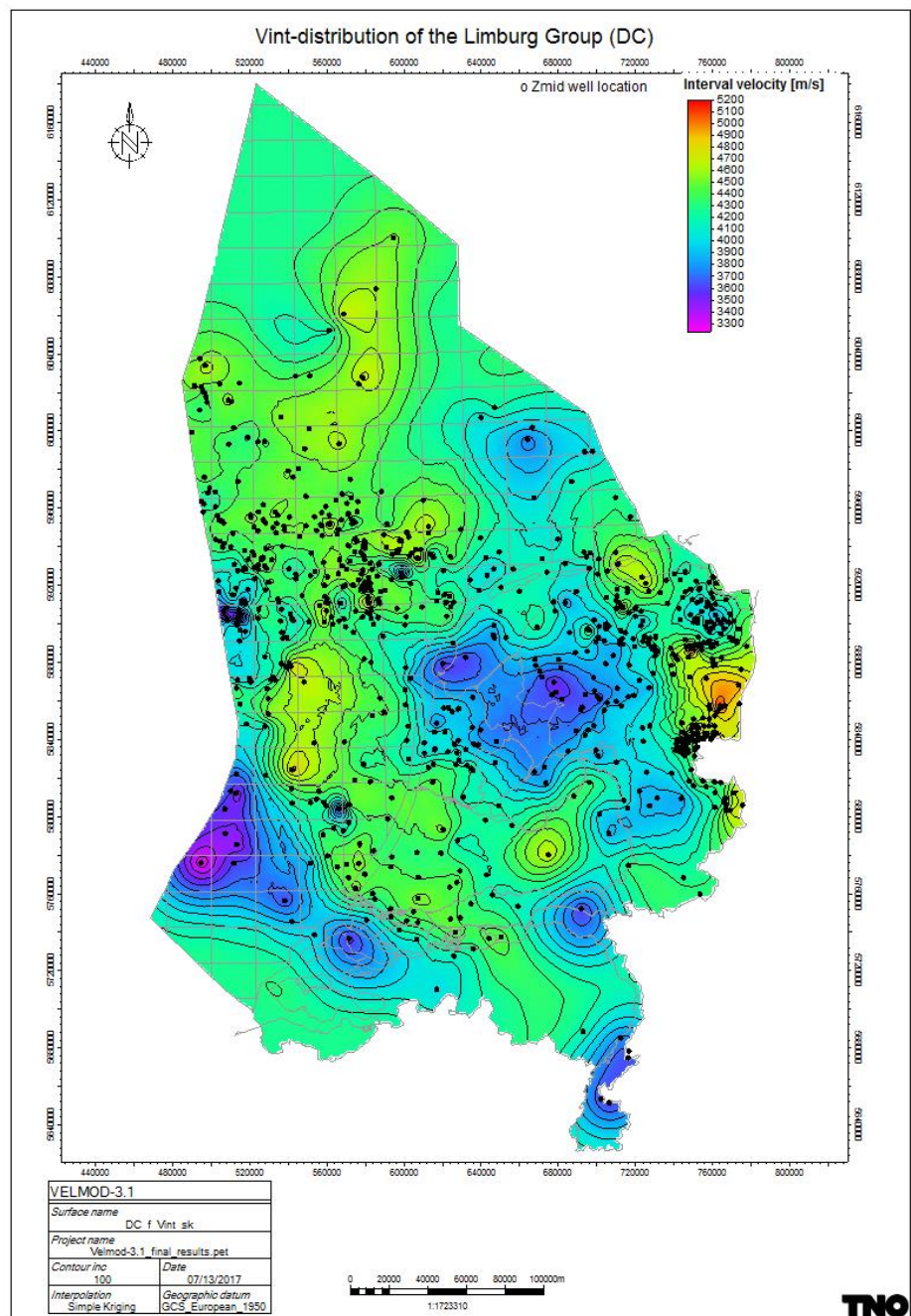


Figure 37  $V_{int}$  distribution of the Lower Germanic Trias Group

Figure 38  $V_{int}$  distribution of the Zechstein Group



Figure 39  $V_{int}$  distribution of the Upper Rotliegend Group

Figure 40  $V_{int}$  distribution of the Limburg Group



### 4.3 Regional $V_0$ distribution maps

Resulting  $V_0$  distribution grids are shown in Figure 41 to Figure 54. The related kriging standard deviation maps are shown in appendix C.

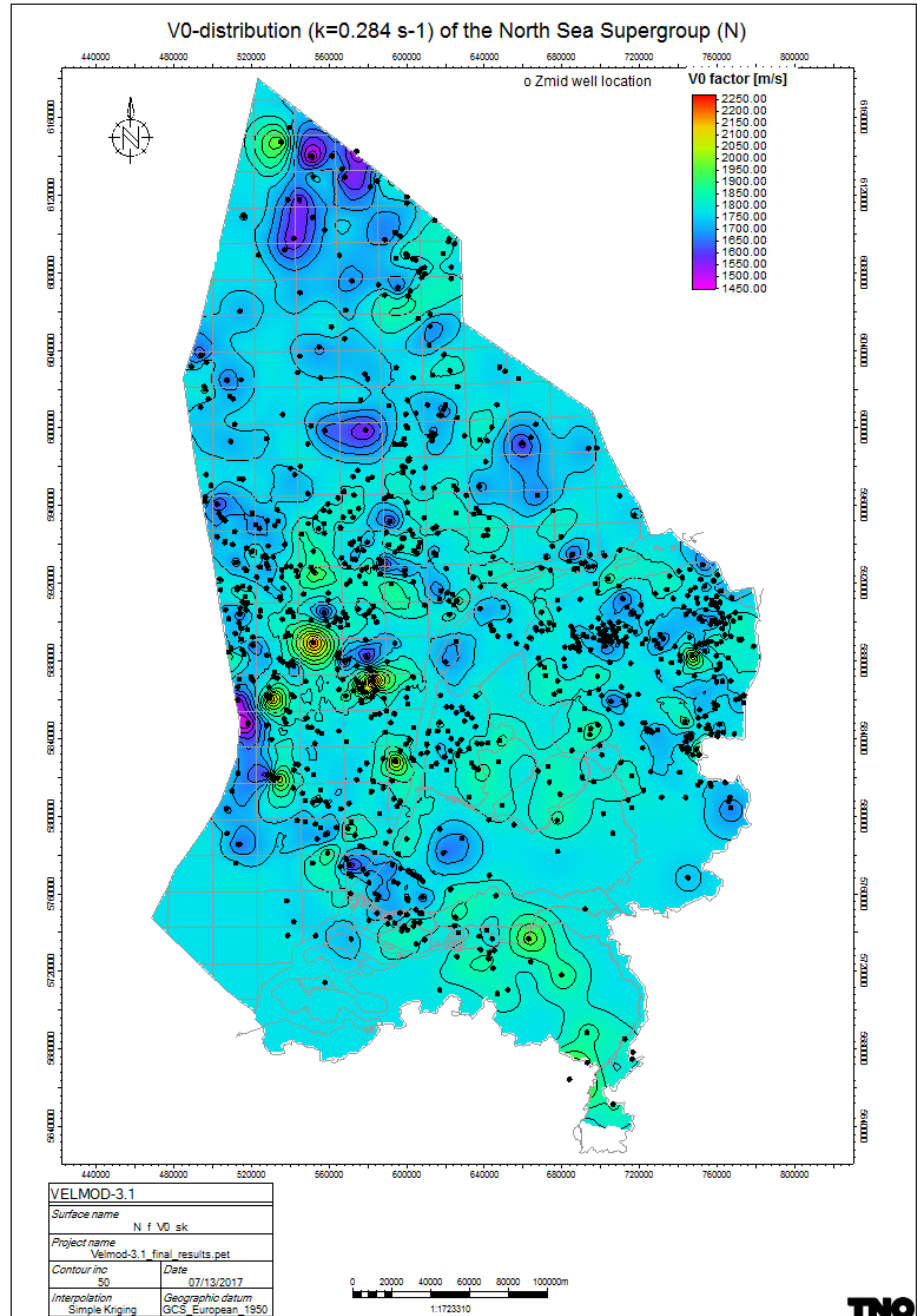


Figure 41  $V_0$  distribution of the North Sea Supergroup

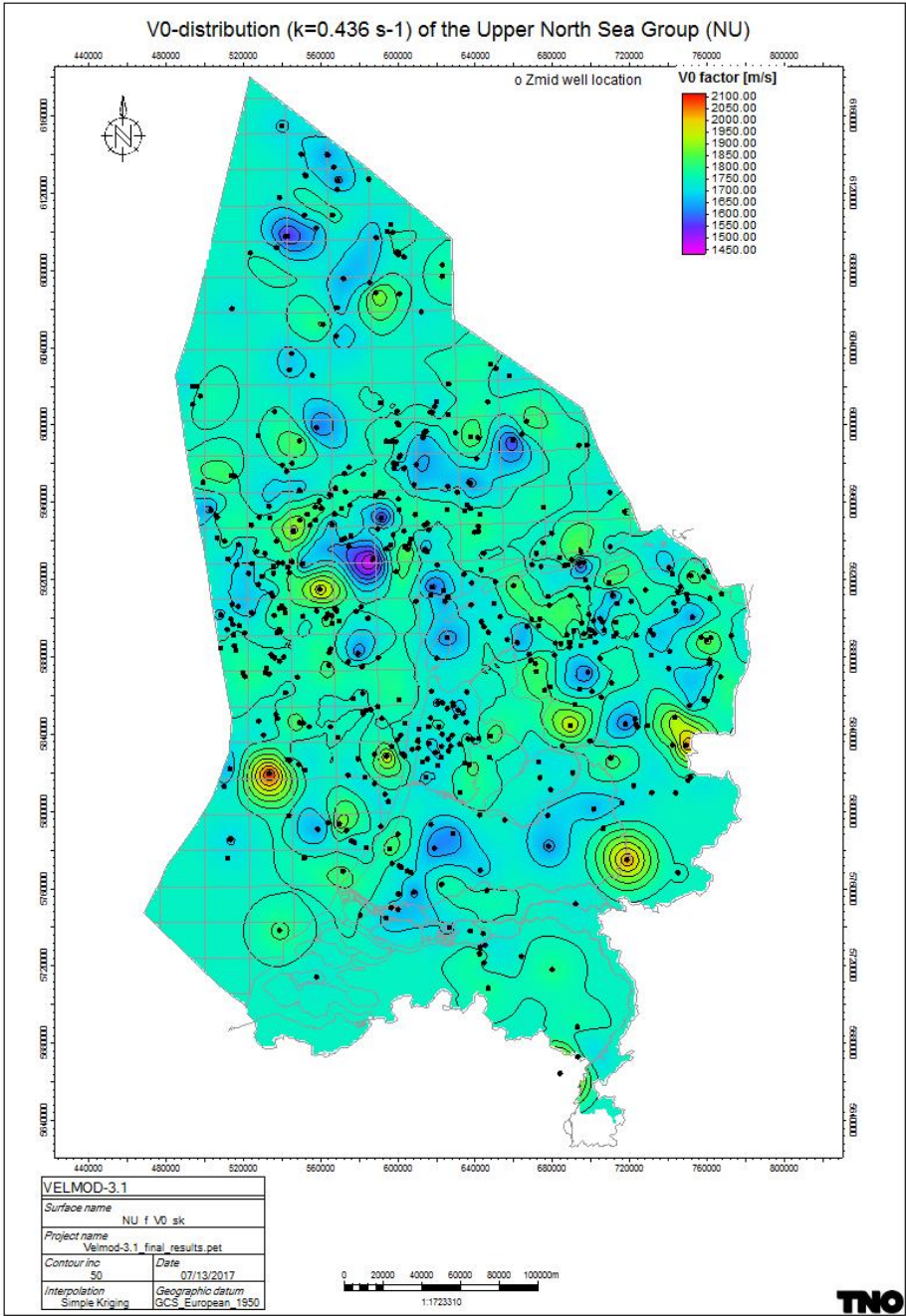


Figure 42  $V_0$  distribution of the Upper North Sea Group

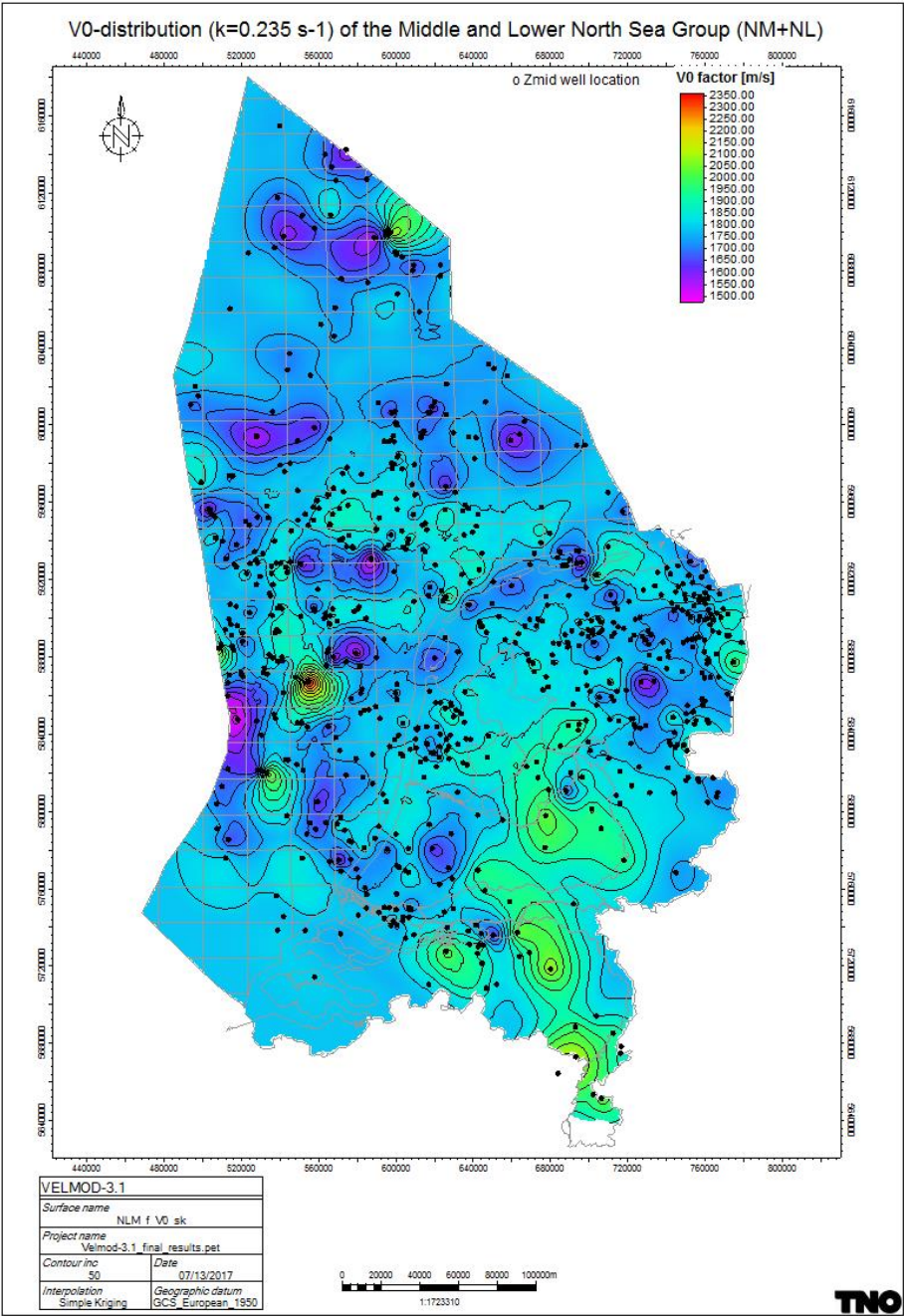


Figure 43  $V_0$  distribution of the Lower and Middle North Sea groups

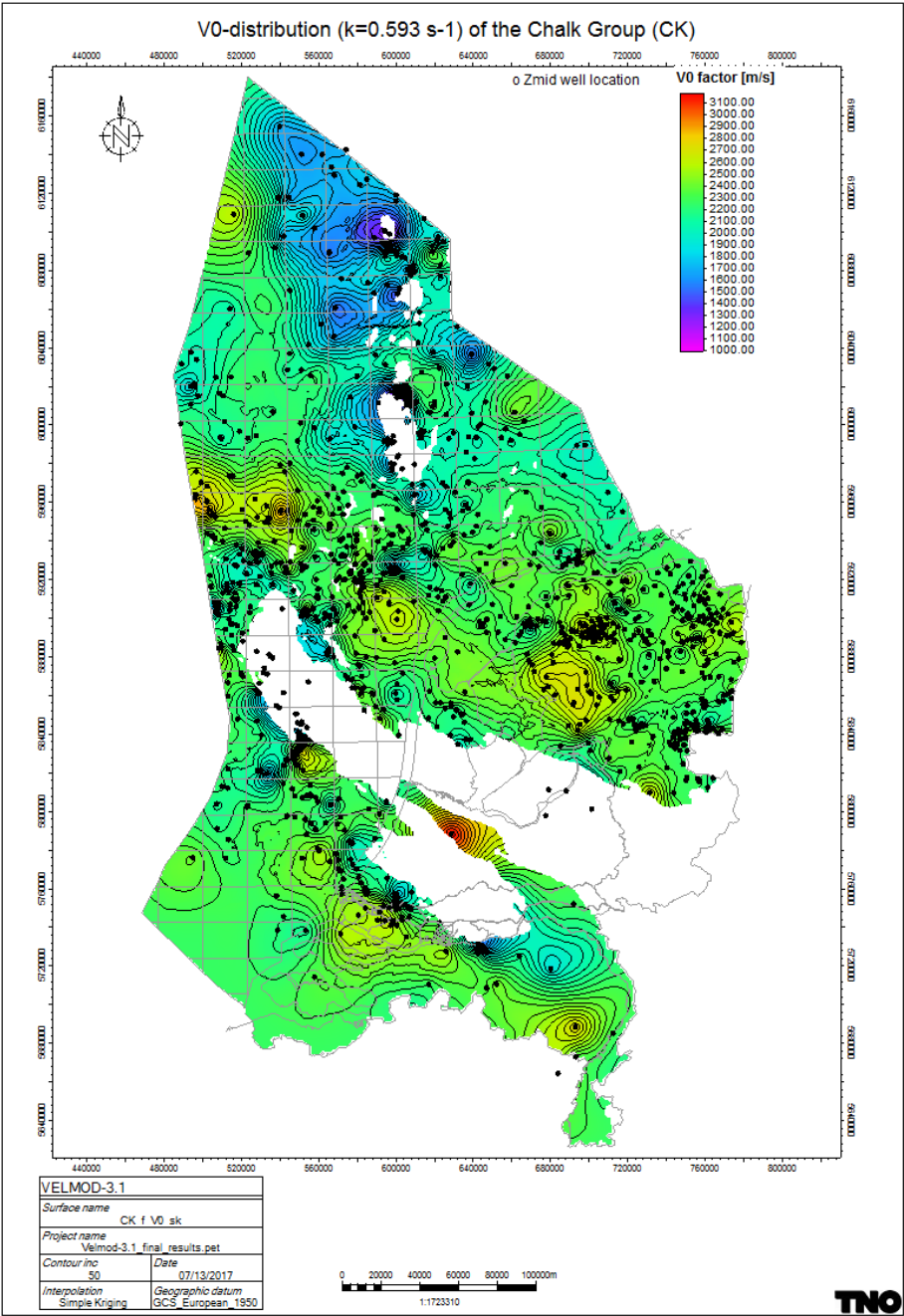


Figure 44  $V_0$  distribution of the Chalk Group



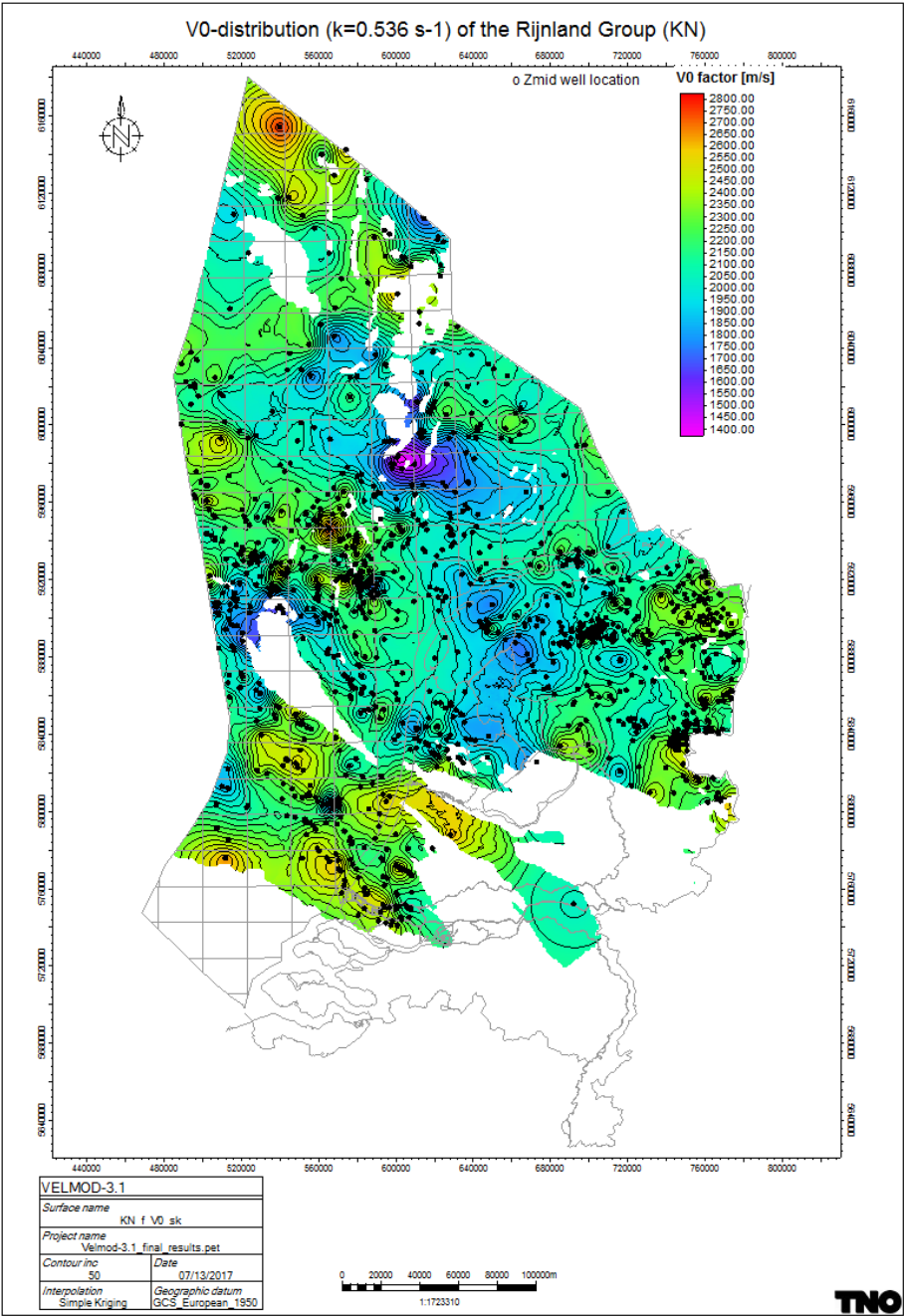


Figure 45  $V_0$  distribution of the Rijnland Group

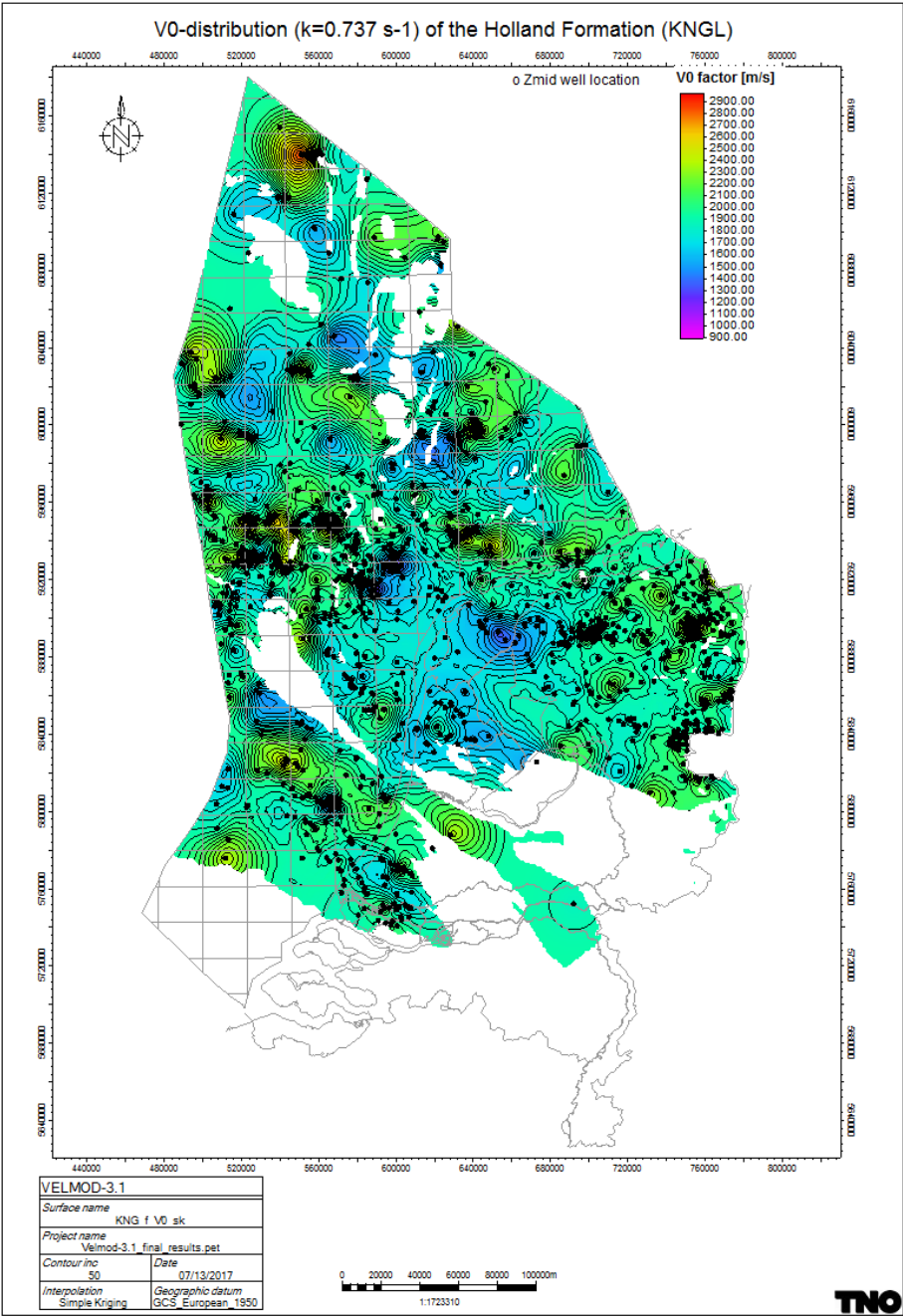


Figure 46  $V_0$  distribution of the Holland Formation

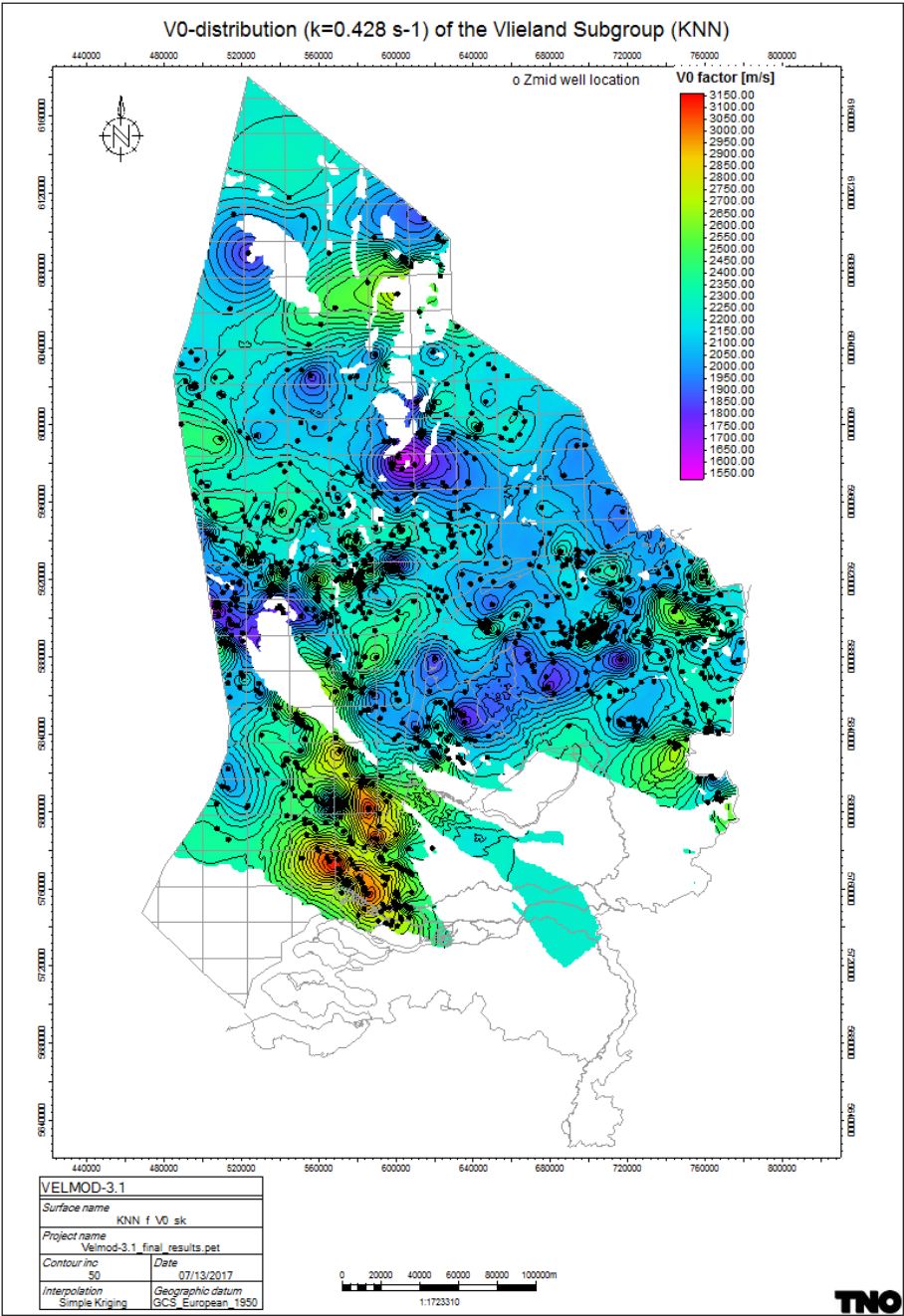


Figure 47  $V_0$  distribution of the Vlieland Subgroup



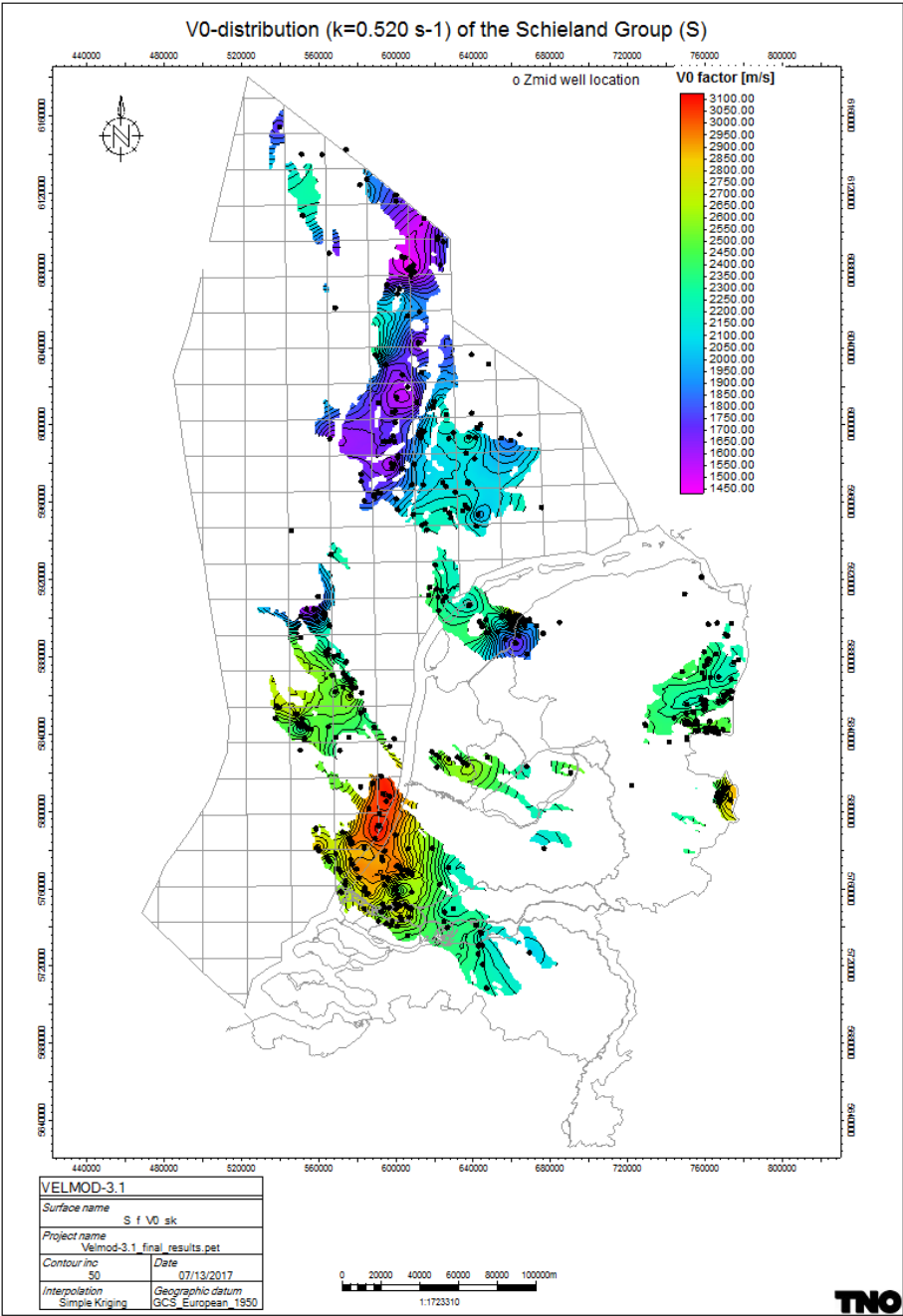


Figure 48  $V_0$  distribution of the Schieland Group

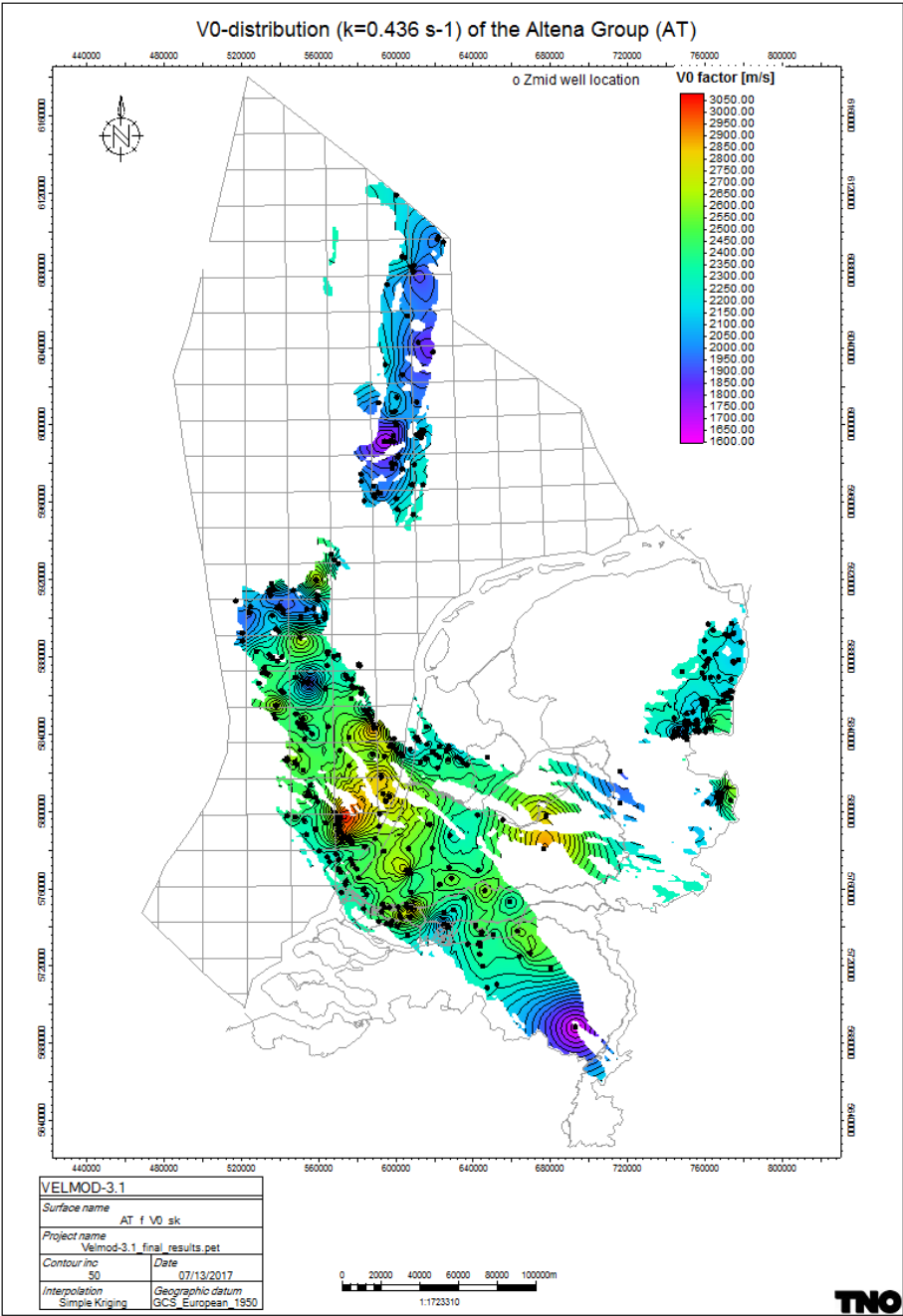


Figure 49  $V_0$  distribution of the Altena Group

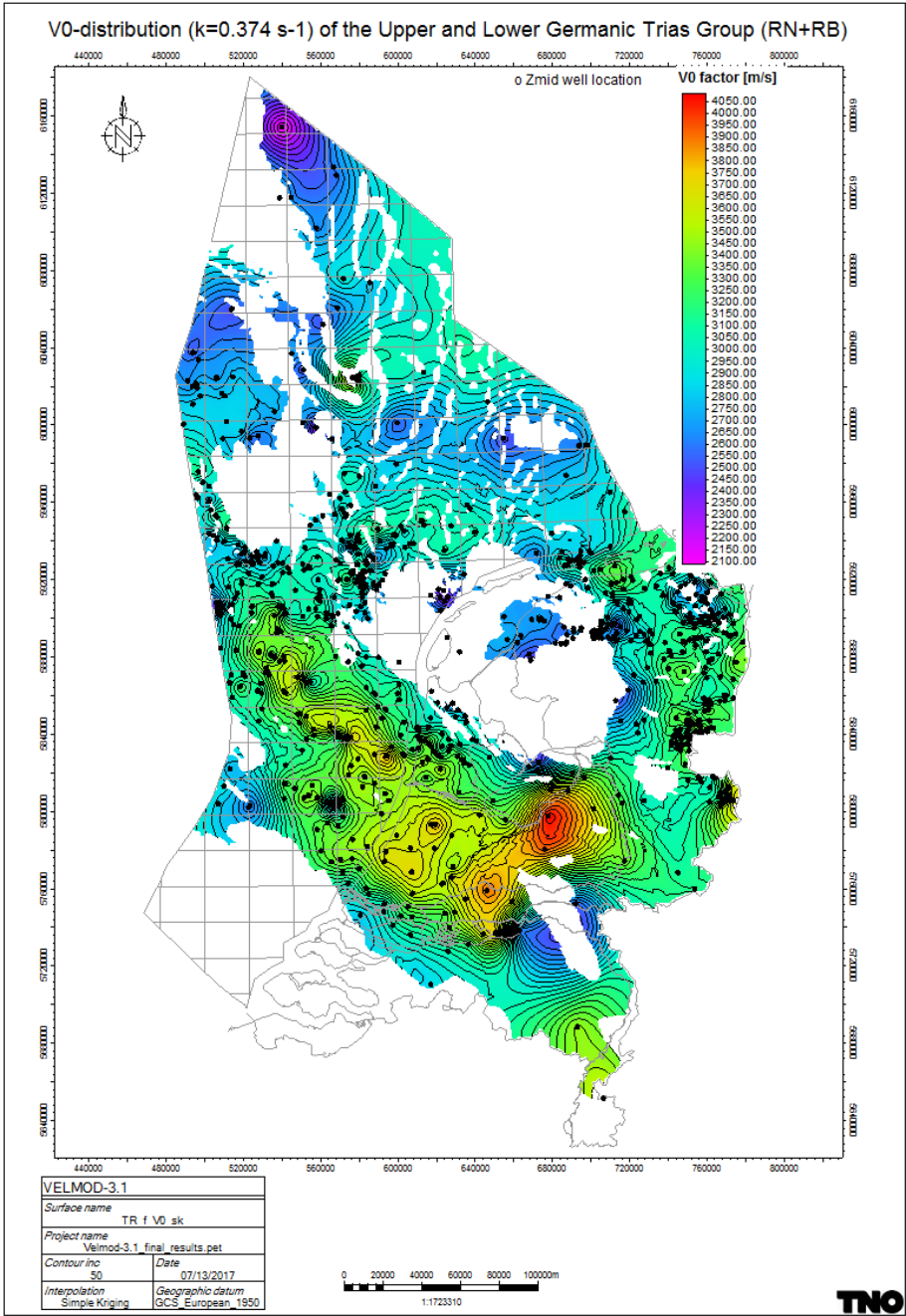
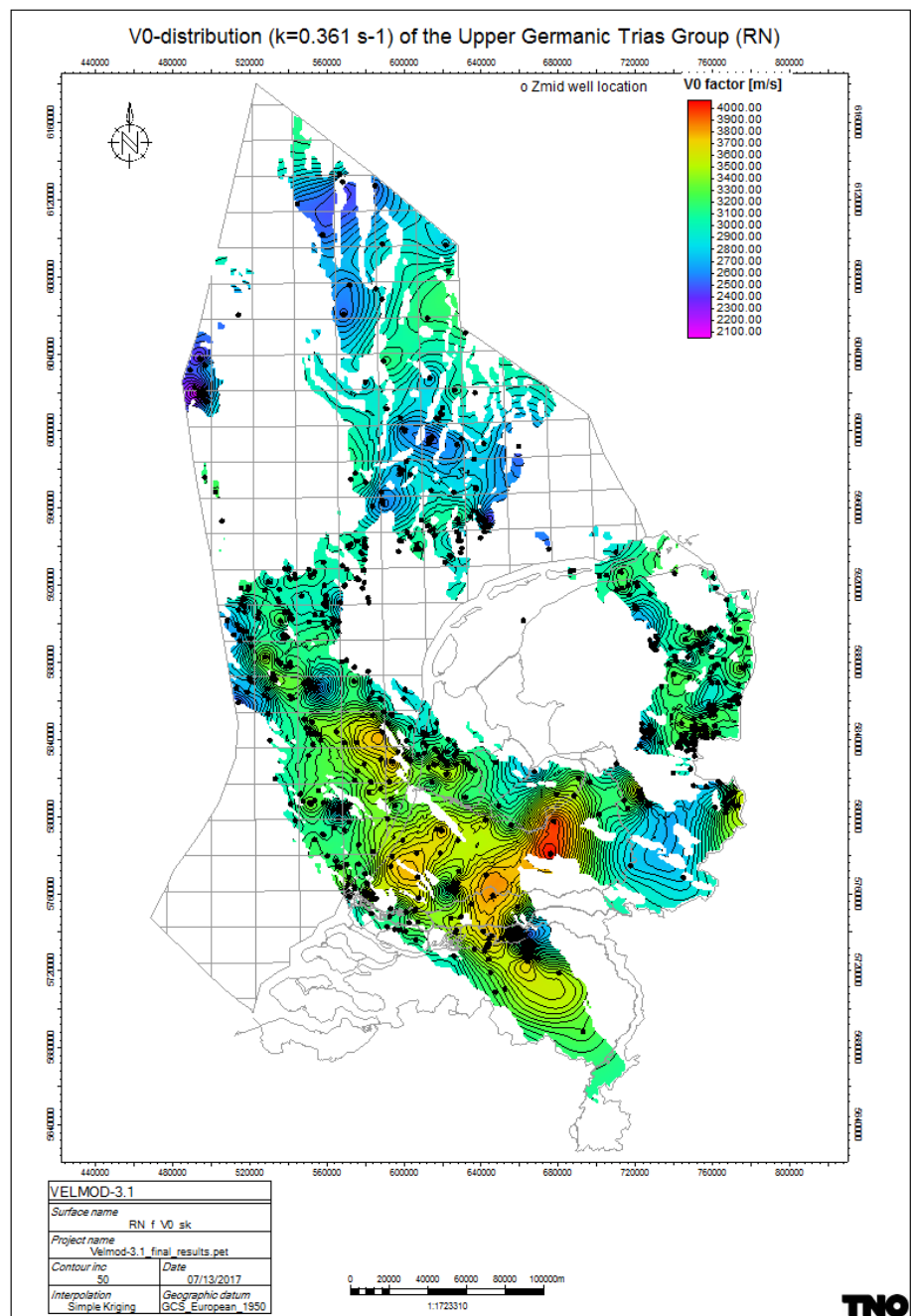
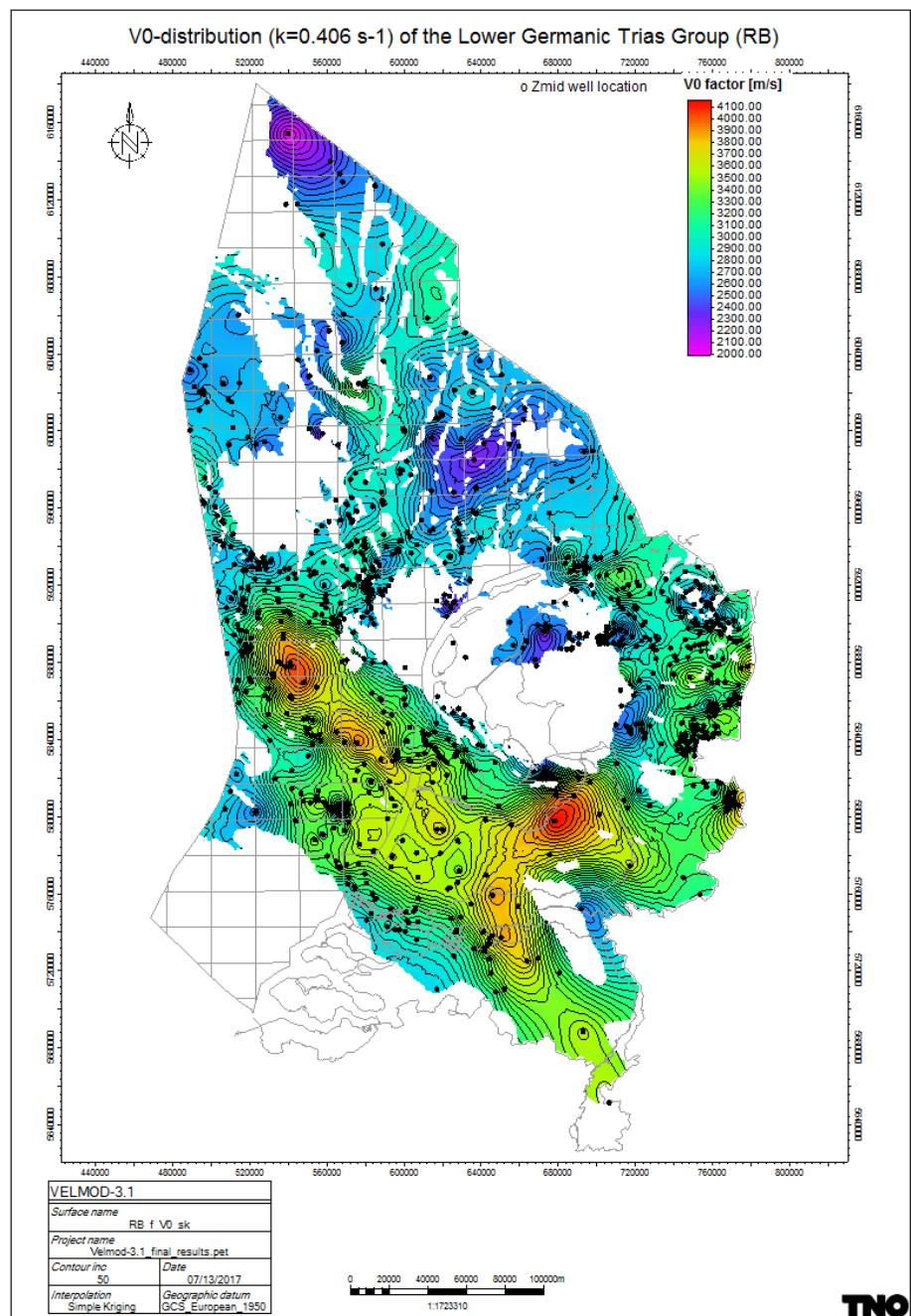
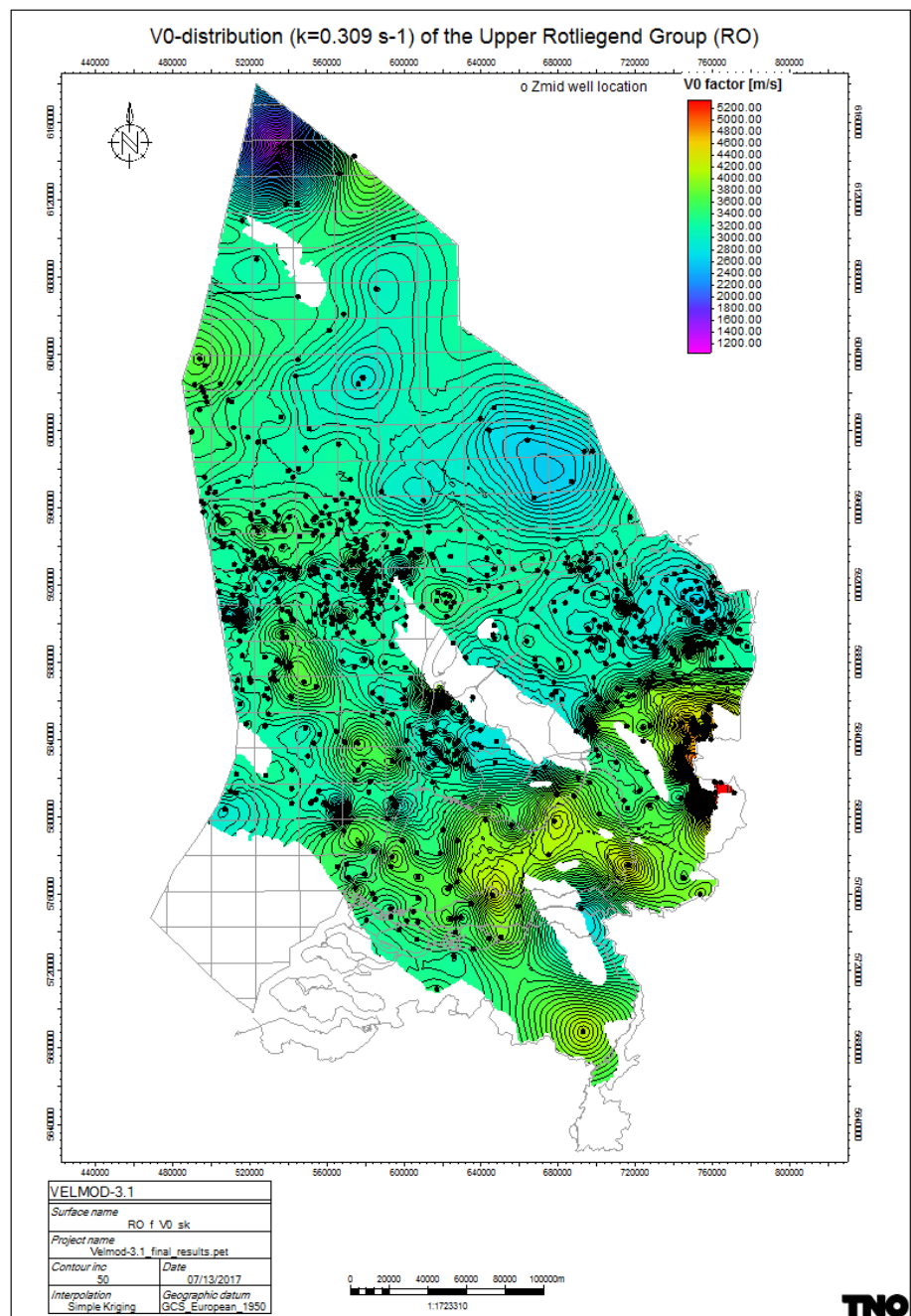


Figure 50  $V_0$  distribution of the Upper and Lower Germanic Trias groups

Figure 51 V<sub>0</sub> distribution of the Upper Germanic Trias Group

Figure 52  $V_0$  distribution of the Lower Germanic Trias Group

Figure 53  $V_0$  distribution of the Upper Rotliegend Group



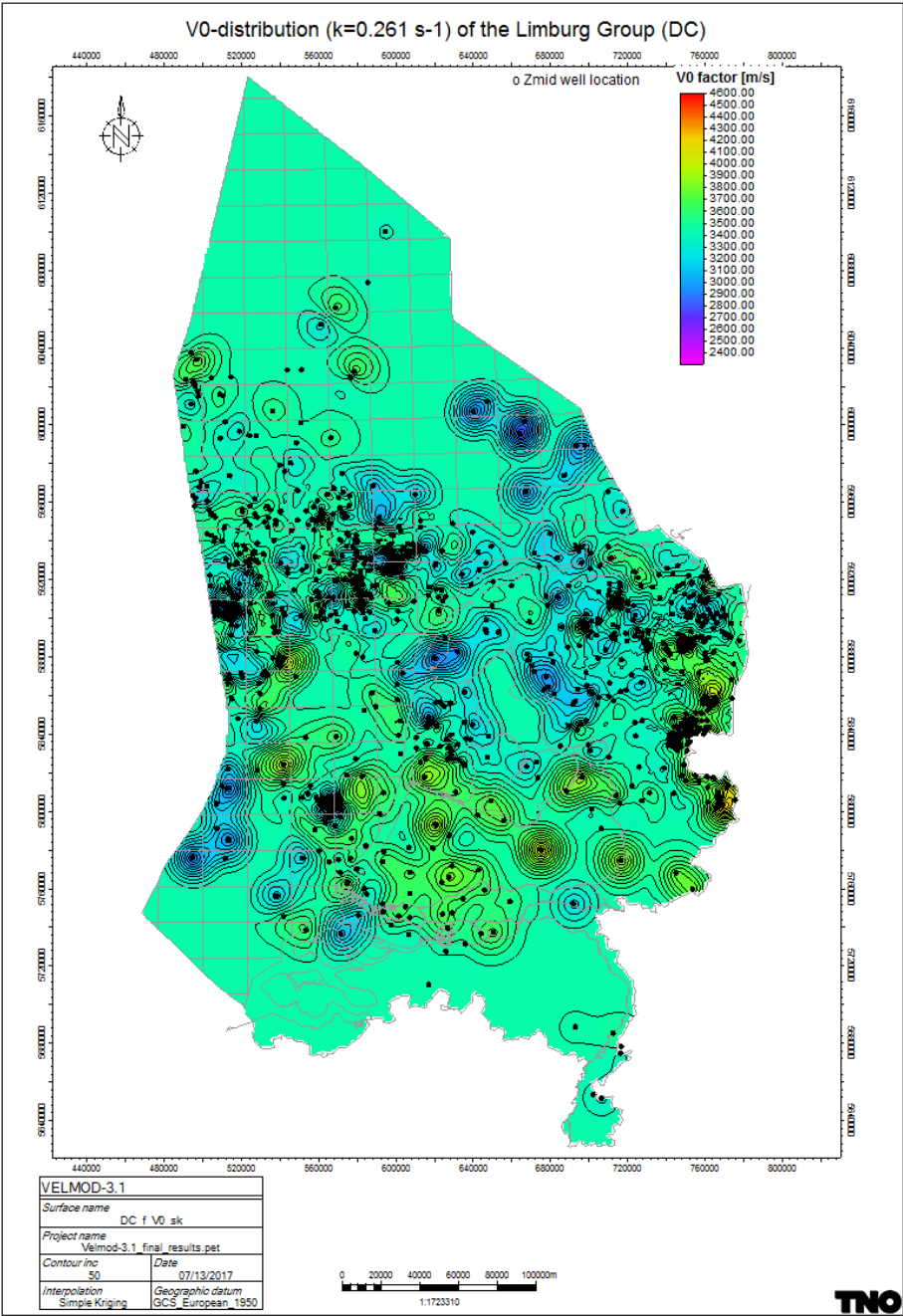


Figure 54  $V_0$  distribution of the Limburg Group

#### 4.4 T/Z pairs

Time-depth pairs were generated from the processed velocity files for the base of every stratigraphic interval. Results are given in Appendix D.

In case the velocity data was not calibrated (so the velocity data does not start at  $Z=0$ ; Figure 55), the velocity of the missing (upper) section was estimated by the  $V_0$ - $k$  parameters.

For comparison, the velocity of the missing section was also estimated by a generalized parameter set where  $V_0 = 1550$  m/s and  $k = 0.6$  s<sup>-1</sup>. This results are annotated as alternative.

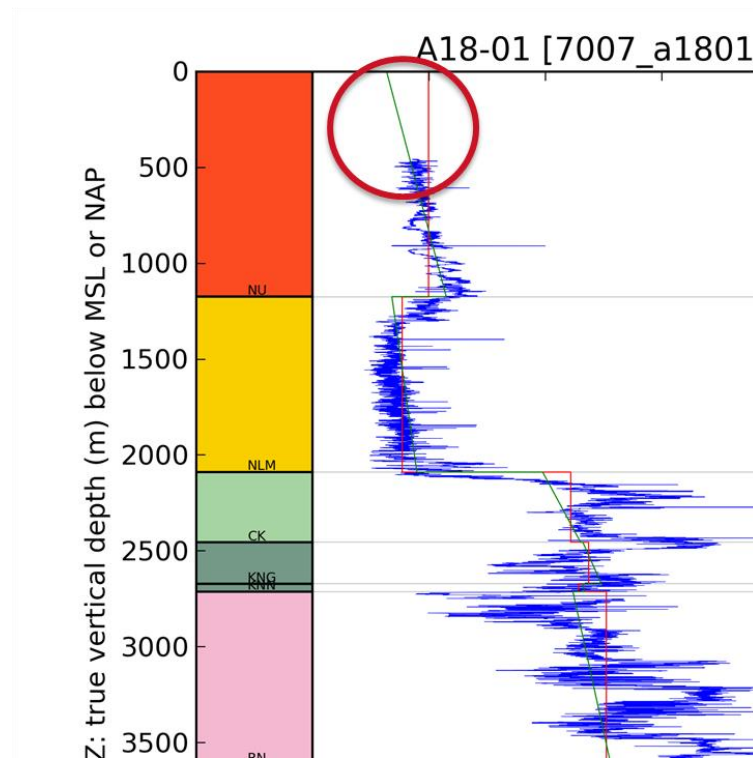


Figure 55 Example of no calibrated velocity dataset, where measurements start at approximately  $z=500$ m. Velocities of the upper section are estimated by the  $V_0$ - $k$  parameters, indicated by the green line.

## 5 Discussion and recommendations

### 5.1 Data reliability

Within VELMOD-3 much effort was given to generate a (semi) automated workflow for processing the velocity, stratigraphic and directional well data. This made it possible to consequently process the 3475 individual velocity data sources of a total of 1642 wells. Well plots of each data set (Appendix A) allows inspection of the data and detection of errors. The selection of a preferred dataset (if multiple datasets were available) per stratigraphic interval was based on a best statistical fit within the complete regional dataset. Although users of VELMOD-3 can select their own preferred dataset for use within geological studies, it is recommended to improve the selection method for the preferred curve in future projects.

### 5.2 Spatial velocity distributions

Limited effort has been given to the modelling of the spatial velocity distributions. For all intervals one single  $k$  and  $V_0$  was derived for the complete regional dataset of the interval (except for the Schieland Group). In several distributions of the  $V_{int}$  (for example for the Chalk Group, figure 57) a bimodal distribution of  $V_{int}$  could be clearly seen and this questions the validity of the use of one single  $k$  and  $V_0$  value.

To analyse if this bimodal interval velocity distribution can be related to differences in the basin structure, the histograms of  $V_{int}$  were differentiated for the structural elements conform the subdivision of Kombrink et al. (2012). Results are given in more detail in Appendix E.

This analysis shows that for the Chalk group the bimodal distribution cannot primarily be explained by differentiation between basin and platform structures. Sediments from the Altena Group were predominantly deposited in the Mesozoic basins. The bimodal character can be explained within the mildly or not inverted basins, where the lower peak can be specifically attributed to the Lower Saxony Basin.

Although the Upper and Lower Germanic Trias Groups do not show a distinct bimodal distribution, the dataset can be differentiated between basins and other structural elements.

Differentiation in structural elements has very limited effect on the Rotliegend distribution. The bimodal character is probably caused by other mechanisms like the lithological composition or the thickness of the unit.

### 5.3 Model parametrization

Analysis of the Schieland Group shows that each of the clustered basins have similar  $k$  values. However, deriving a general  $k$ -value for the complete regional dataset leads to a lower  $k$  value, and so underestimation of velocity increase with depth. It's recommended in future projects to explore the possibility of deriving  $k$ -values for regional subdivided areas for all stratigraphic intervals.

In addition to this,  $k$  is based on the linear regression of the interval velocity on mid-depth, estimated by ordinary least squares. Given the fact that the resulting velocity model will be used to convert from time to depth and vice-versa, a more robust regression is probably more appropriate. Therefore it is recommended to explore

the use of different regression methods like: *reduced major axis regression*, *median fit* or *principal component regression*.

#### 5.4 Velocity model

The  $V_0$ -k model was validated by time-depth conversion of the ongoing regional seismic interpretation and mapping program (DGM-deep V5), where for every borehole, also for boreholes without velocity information, statistics on depth residuals are compiled.

Bulls-eyes in the resulting velocity grids are examined, as a activity within the DGMdeep V5 proces, on possible inconsistencies in a) stratigraphic interpretation within the borehole, b) seismic well tie, c) well velocity and d) local geological aspects.

The  $V_0$ -k model is for TNO the preferred model for regional time-depth conversion. Besides the  $V_0$ -k model, two  $V_{\text{int}}$  models were constructed and described in this report. The  $V_{\text{int}}$  model (especially the  $V_{\text{int}}$  *simple kriging*) is a pure representation of the interval velocities measured in the boreholes, and is not subject to model assumptions made in the  $V_0$ -k model. It therefore can help a geologist with the validation of a velocity model and resulting time-depth conversion.

#### 5.5 Geological aspects

The primary goal of VELMOD-3 was the construction of a regional velocity model for the use of time-depth conversion of regional seismic interpreted horizons. However, the  $V_0$ -distributions for a number of layers can be interpreted in geological terms of for example: overpressured pore fluids, burial anomalies or variations in lithology/reservoir properties. The spatial interpolation of the velocity data can be improved by incorporating regional knowledge on overpressured areas and areas subject to phases with major uplift.

## 6 References

Japsen, P., 1993. Influence of lithology and Neogene uplift on seismic velocities in Denmark: implications for depth conversion of maps. American Association of Petroleum Geologists Bulletin 77, No.2: 194-211.

Kombrink, H., Doornenbal, J.C., Duin, E.J.T., den Dulk, M., van Gessel, S.F., ten Veen, J.H. & Witmans, N., 2012. New insights into the geological structure of the Netherlands; results of a detailed mapping project. Netherlands Journal of Geosciences 91-4, 419 - 446.

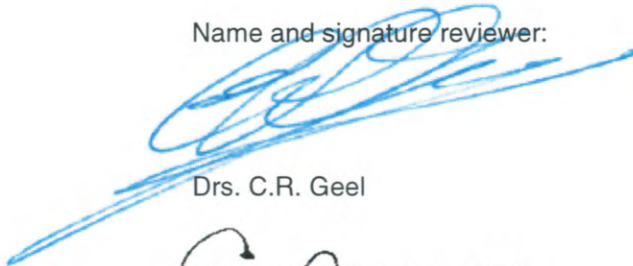
Van Adrichem Boogaert, H.A. & Kouwe, W.F.P., 1993-1997 (eds). Stratigraphic nomenclature of the Netherlands, revision and update by RGD and NOGEPa, Mededelingen Rijks Geologische Dienst, nr. 50.

Van Dalfsen, W., van Gessel, S.F. & Doornenbal, J.C., 2007. Velmod-2 Joint Industry Project. TNO report 2007-U-R1272C.

## 7 Signature

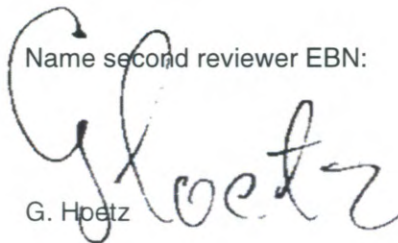
Name and address of the principal:

Name and signature reviewer:

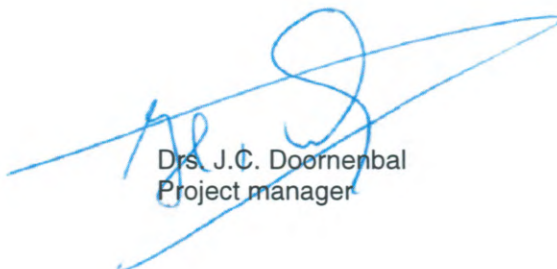


Drs. C.R. Geel

Name second reviewer EBN:



G. Hoetz



Drs. J.C. Doornenbal  
Project manager



Dr. M.J. van der Meulen  
Research manager



## A Velocity borehole data files

For all processed velocity files, plots are generated with stratigraphic information. An example is given in Figure 56.

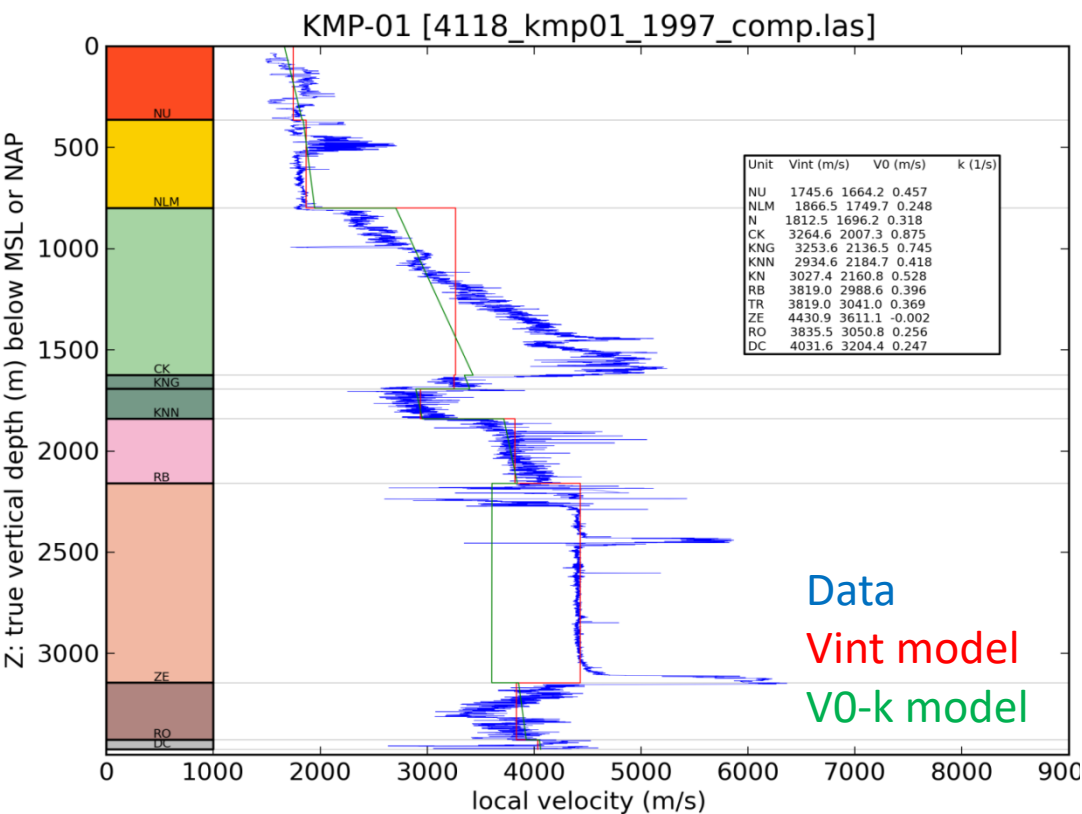


Figure 56 Example of velocity borehole file. Stratigraphic subdivision is given in the left colorbar. Interval velocity model is plotted in red and V0-k velocity model is plotted in green overlain by the source data (blue).

## B Velocity model well results

See results file: *velmod3\_all\_welldata.xlsx*

The headers of the column names in this Excel-file are described in Table 4

**Table 4 Column description of velmod3\_all\_welldata.xlsx**

Column name	Description
<b>short_nm</b>	well name
<b>strat_cd</b>	stratigraphic interval
<b>dataset</b>	file name of data
<b>use_status</b>	False = discard by QC
<b>filtered</b>	True = used for regression line
<b>preferred</b>	True = preferred dataset for well/strat combi
<b>xmid</b>	x coord mid depth
<b>ymid</b>	y coord mid depth
<b>zmid</b>	mid depth of strat interval
<b>dz</b>	thickness stat interval
<b>matching_interval</b>	coverage of data compared to strat interval
<b>vint</b>	Interval velocity (dz/dt)
<b>vmean</b>	average velocity (average of velocity values)
<b>vsd</b>	standard deviation of velocity (vmean)
<b>count</b>	nr of datapoints
<b>variation</b>	variance of velocity (vmean)
<b>bin_mode</b>	mode of binned dataset
<b>bin_freq</b>	frequentie od mode bin
<b>bin_size</b>	in m/s
<b>v0global</b>	V0 global
<b>v0local</b>	V0 local
<b>v0local_basefit</b>	V0 local, error at base level was minimized
<b>kglobal</b>	k global
<b>rmslocal</b>	rms error of V0 local fit
<b>dt_well</b>	delta time in well
<b>dt_seis</b>	delta time from seismic interpretation
<b>dz_vint</b>	model residuals Vint model (depth error)
<b>dz_v0k</b>	model residuals V0-k model (depth error)
<b>dz_v0k_basefit</b>	model residuals V0-k basefit model (depth error)
<b>is_calibrated</b>	velocity data starts at z=0
<b>has_truncated_base</b>	missing velocity data in lower part stratigraphic section
<b>has_truncated_top</b>	missing velocity data in upper part stratigraphic section
<b>vel_type</b>	type of data used (sonic/cs/tz)
<b>vel_src</b>	source data type (las curve)
<b>flag</b>	remarks
<b>duplicate</b>	marked as duplicate x,y values

**Table 5 Description of velocity source data types used**

<b>vel_src</b>	<b>vel_type</b>	<b>refers to the type of velocity measurement</b>
dt	son	unspecified sonic log
tw	tw	two way time derived form unspeciefied source (checkshots)
ac	son	acoustic log
son	son	unspecified sonic log
timc	owt	corrected travel time
dtc	son	corrected sonic log
twotim	tw	two way time derived form unspeciefied source
vel	vel	velocity derived form unspeciefied source
owt	owt	one way time derived form unspeciefied source
dtccal	son	calibrated (compressional) sonic log
dtc_cal	son	calibrated corrected sonic log
dtl	son	long spaced sonic
dtcl	son	unspecified sonic log
dtlf	son	long spaced sonic far
dtln	son	long spaced sonic near
dtco	son	(compressional) sonic log
intt	son	interval transist time
dtc_ed_cal	son	calibrated corrected sonic log, edited
dtc_ed	son	corrected sonic log, edited
dtc_edt_cal_winz	son	calibrated corrected sonic log, edited
dtc_m-s	son	corrected sonic log
dtc_cal_ssl	son	calibrated corrected sonic log
dtin	son	delta t input
dt_cal_winz	son	calibrated sonic log
dtc_edited	son	corrected sonic log, edited
dtc_cal_winz	son	calibrated corrected sonic log
dtc_edt	son	corrected sonic log, edited
dt_mmk	son	unspecified sonic log
dtc cal	son	calibrated corrected sonic log
dtc-cal vel	son	calibrated corrected sonic log

**Table 6 Description of velocity measurement type**

<b>vel_type</b>	<b>refers to unit of velocity measurement</b>
son	sonic log [us/ft]
owt	one way travel time [s, or ms]
tw	two way travel time [s, or ms]
vel	velocity [m/s]

## C Vint, $V_0$ & kriging standard deviation grids

De grids zijn te vinden op [nlog.nl](http://nlog.nl)

## D T/Z pairs

See results file: velmod3\_all\_tz\_basefit.xlsx

The headers of the column names in this Excel-file are described in **Table 7**.

**Table 7** Description of the column names of velmod3\_all\_tz\_basefit.xlsx

Column name	Description
<b>short_nm</b>	well name
<b>strat_base_cd</b>	stratigraphic interval code
<b>x</b>	x coordinate
<b>y</b>	y coordinate
<b>z</b>	depth of base stratigraphic interval
<b>t</b>	time of base stratigraphic interval
<b>t_alt</b>	alternative time of base stratigraphic interval
<b>remark</b>	remarks
<b>dataset</b>	file name of dataset
<b>preferred</b>	True = preferred dataset for well/stratigraphy combination
<b>calibrated</b>	velocity data starts at z=0

## E Analysis of regional Vint variations

To analyse the effect of different structural elements on the interval velocity distribution, the histograms of Vint were differentiated for the structural elements conform the subdivision of Kombrink et al. (2012).

Differentiation in the following types was applied:

- High
- Platform (Cretaceous or Paleogene on top of Zechstein)
- Platform (Cretaceous or Paleogene on top of Triassic)
- Basin (Strongly inverted)
- Basin (Mildly or not inverted)

### E.1 Chalk Group (CK)

The bimodal character of the Chalk Vint distribution cannot primary be explained by the separation in basins and other structural element types. The interval velocity in the basins has a lower average (2000 - 4250) compared to the platforms (2000 - 5000). Within the platform subset, the interval velocity is on average higher (3250-5000) where Cretaceous or Paleogene is directly overlaying the Zechstein.

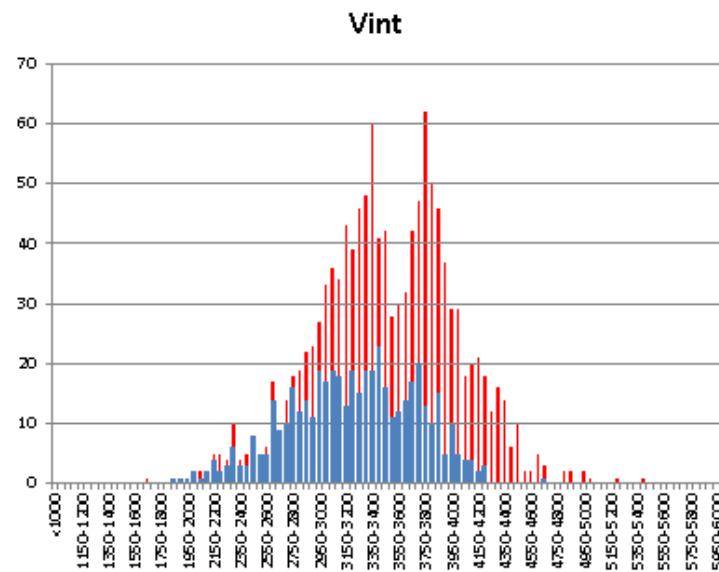


Figure 57 Interval velocity distribution of basins (blue) compared to the total distribution (red).



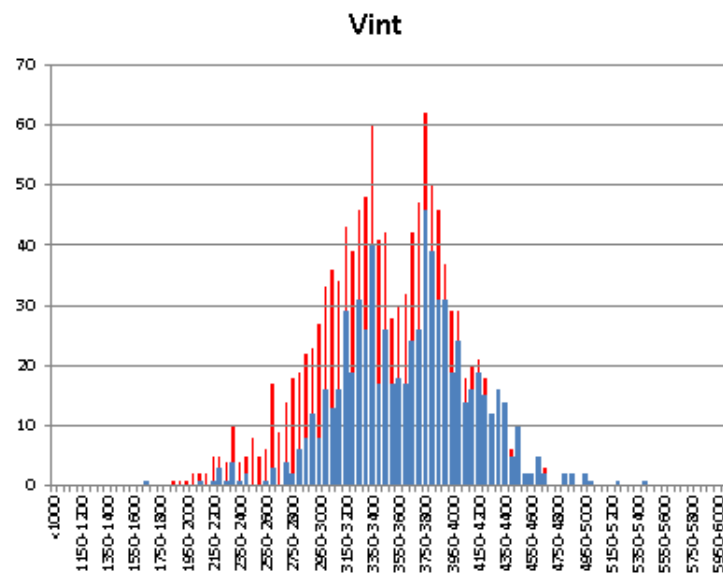


Figure 58 Interval velocity distribution of all platforms (blue) compared to the total distribution (red).

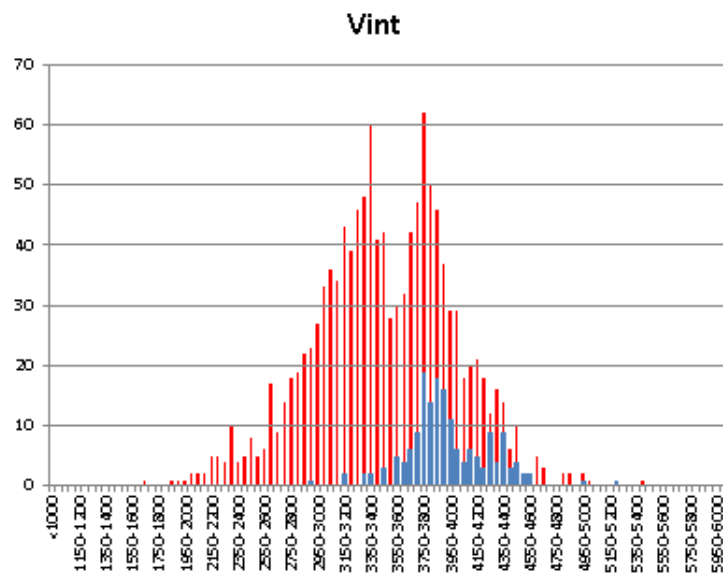


Figure 59 Interval velocity distribution of platforms- Cretaceous or Paleogene on top of Zechstein (blue) compared to the total distribution (red).

## E.2 Altena Group (AT)

The sediments of the Altena Group are mostly present in the basins. The bimodal character can be explained within the mildly or not inverted basins. The lower peak in the bimodal Vint distribution can be attributed to the Lower Saxony Basin. The strongly inverted basins do not show a bimodal distribution.

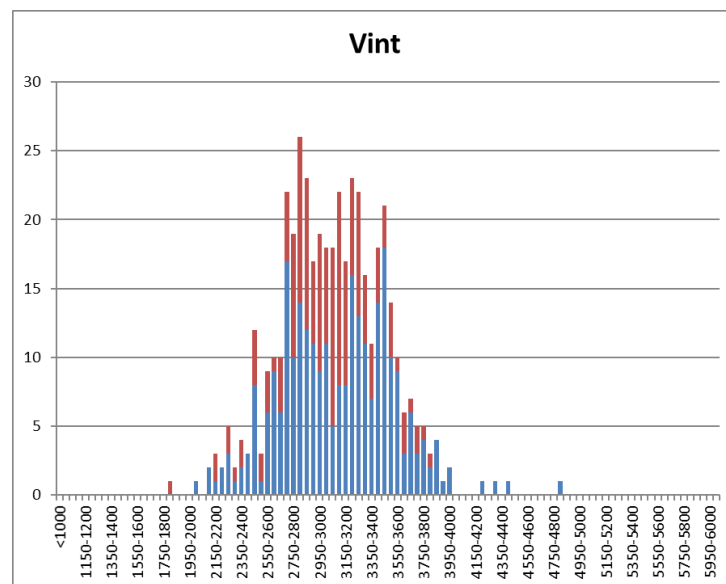


Figure 60 Interval velocity distribution of basins- Mildly or not inverted (blue) compared to the total distribution (red).

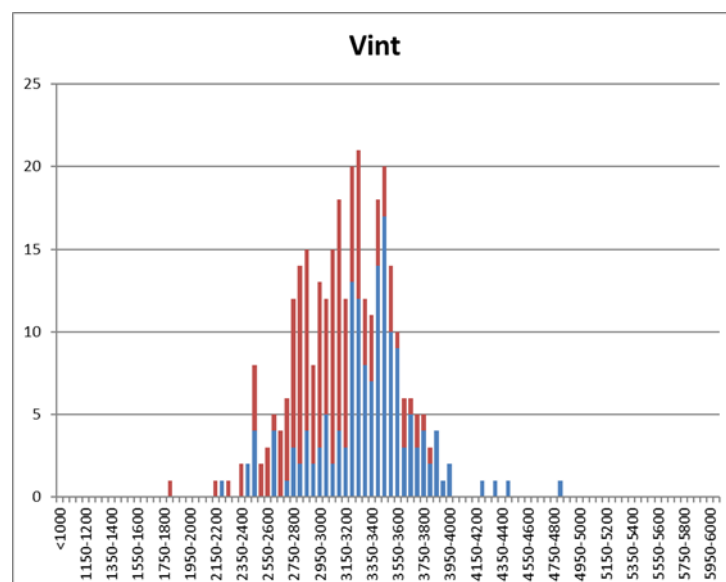


Figure 61 Interval velocity distribution of basins- Mildly or not inverted, excluding the Lower Saxony Basin (blue) compared to the total distribution (red).

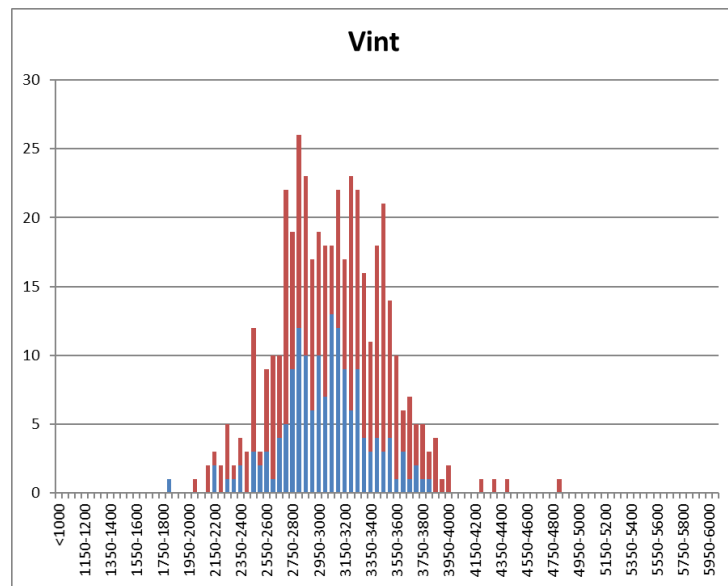


Figure 62 Interval velocity distribution of basins- Strongly inverted (blue) compared to the total distribution (red).

### E.3 Upper and Lower Germanic Trias Group (RN+RB)

The differentiation between basins and other structural elements is inversely proportional with the Chalk distribution. The Triassic sediments in the basins have a average higher Vint (3000-5000) than the platforms (2750-4750). Within the platform subset it is difficult to further differentiate.

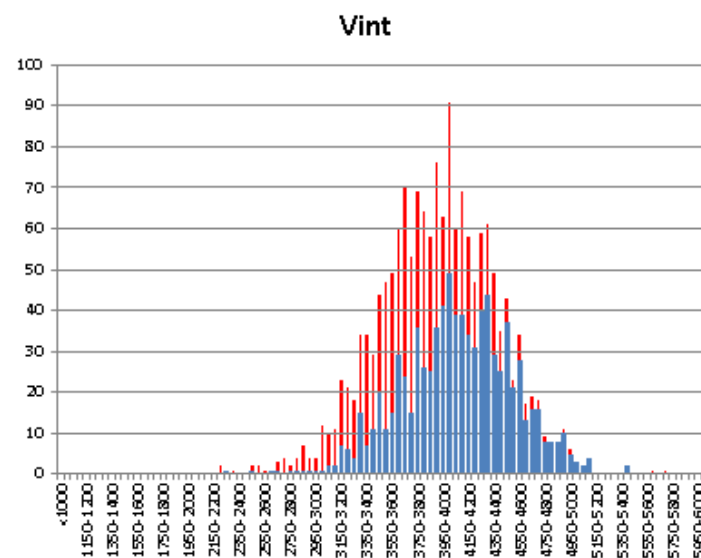


Figure 63 Interval velocity distribution of basins (blue) compared to the total distribution (red).

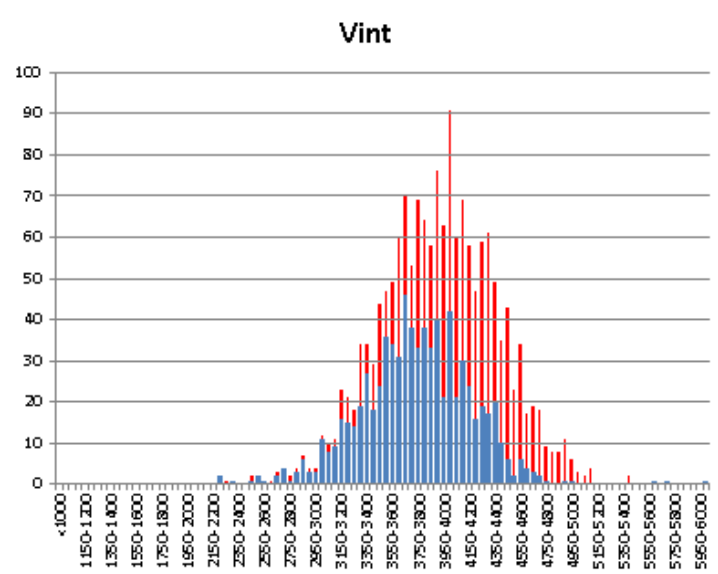


Figure 64 Interval velocity distribution of platforms (blue) compared to the total distribution (red).

## E.4 Upper Rotliegend Group (RO)

Differentiation in structural element has very limited effect on the Rotliegend distribution. The bimodal character is probably caused by the lithological composition or the thickness of the unit. Vint values above 5500 m/s are caused by saltplugging of the Rotliegend sands.

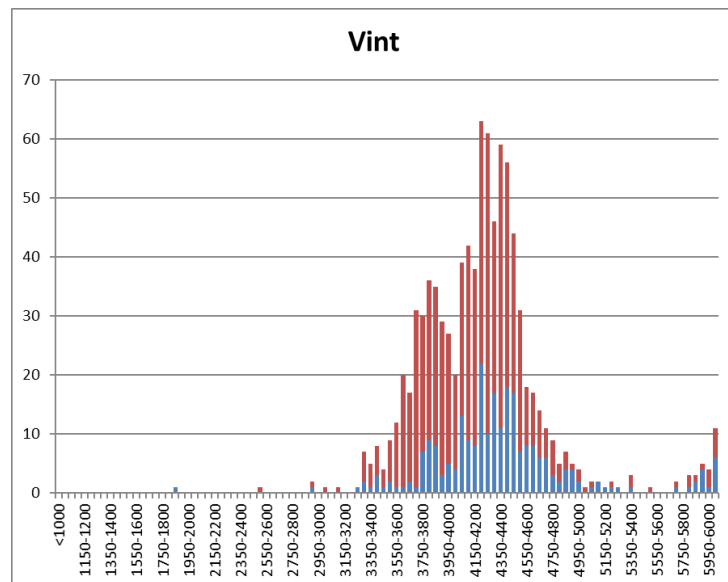


Figure 65 Interval velocity distribution of basins (blue) compared to the total distribution (red).

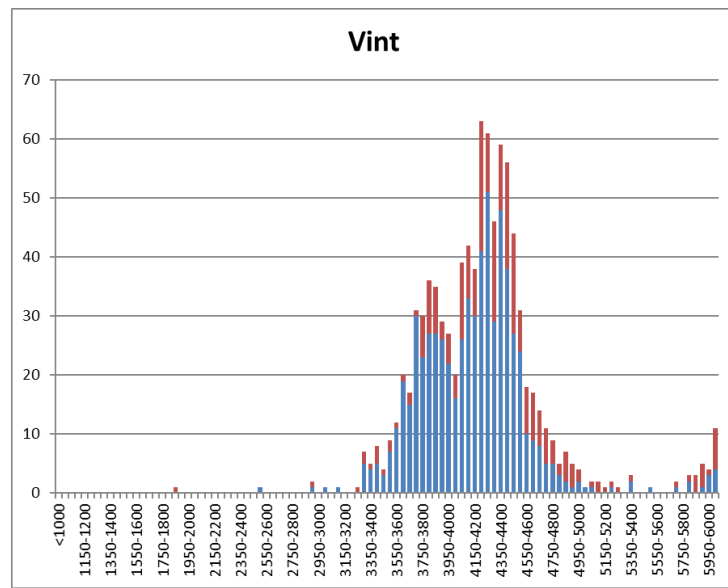


Figure 66 Interval velocity distribution of platforms (blue) compared to the total distribution (red).